Structures 70 (2024) 107543

Contents lists available at ScienceDirect

Structures

journal homepage: www.elsevier.com/locate/structures

Machine learning-based probabilistic predictions for Concrete Filled Steel Tube (CFST) column axial capacity

Dade Lai [a], Jingyu Wei [b], Alessandro Contento [c], Junqing Xue [c], Bruno Briseghella [c], Tommaso Albanesi [d], Cristoforo Demartino [d,*]

[a] College of Transportation and Civil Engineering, Fujian Agriculture and Forestry University, Fuzhou, 35010 Fujian, PR China
[b] College of Civil Engineering and Architecture, Zhejiang University, Hangzhou, 310058 Zhejiang, PR China
[c] College of Civil Engineering, Fuzhou University, Fuzhou, 35010 Fujian, PR China
[d] Department of Architecture, Roma Tre University, Largo G. B. Marzi 10, Rome, 00153, Italy

ARTICLE INFO

Keywords:
Probabilistic machine learning
Concrete Filled Steel Tube (CFST)
Axial compressive capacity
Natural Gradient Boosting (NGBoost)
SHapley Additive exPlanations (SHAP)

ABSTRACT

This study presents a novel probabilistic machine learning (ML) approach using Natural Gradient Boosting (NGBoost) to predict the axial compressive capacity of Concrete Filled Steel Tube (CFST) columns. Leveraging a comprehensive dataset of 1,127 experimentally tested CFST specimens under axial compressive loads, we compare the performance of various ML algorithms. These include deterministic models like eXtreme Gradient Boosting (XGBoost) and Artificial Neural Networks (ANN), and probabilistic models such as XGBoost-Distribution (XGBD) and NGBoost. The NGBoost model, which employs Normal and LogNormal distributions to account for uncertainties in input data, demonstrates superior predictive accuracy and robustness. SHapley Additive exPlanations (SHAP) are utilized to interpret the influence of input features, providing insights into the relative importance of different structural parameters. The predictive performance of the NGBoost model with LogNormal distribution is benchmarked against existing design codes, including Eurocode 4, ANSI/AISC 360-22 AS/NZS 2327, and Chinese Standard (GB50936-2014), showcasing its enhanced accuracy and reliability. This approach not only improves predictive performances but also integrates uncertainty quantification, making it highly suitable for design applications in Civil Engineering where understanding the variability in the structural behavior is crucial.

1. Introduction

The development of modern infrastructure is increasingly oriented towards large-scale, high-rise, and long-span structures, which pose significant challenges for building materials and structural designs [1]. Traditional Reinforced Concrete (RC) structures struggle to meet these demands due to their relatively low strength and considerable self-weight, especially when large sectional sizes are required. Concrete Filled Steel Tube (CFST) structures, which combine the benefits of both concrete and steel, have emerged as a popular solution across various engineering fields, including bridge, coastal, and mountainous engineering [2–9]. The inner concrete in CFST columns prevents premature local buckling of the outer steel tube, while the steel tube acts as a formwork for the concrete, enhancing the overall structural integrity [10].

The axial compressive capacity of CFST columns is crucial for their effective use in bearing axial loads. Numerous experimental tests have been conducted to evaluate this capacity, as documented in several studies (e.g., [11–13]). These tests highlight the superior axial compressive performance of CFST columns compared to concrete alone. The significant enhancement in axial capacity is attributed to the confinement effect provided by the steel tube [10,14]. CFST columns can be constructed with various cross-sections, such as circular, rectangular, and square. However, circular sections are preferred for achieving higher axial load-carrying capacity and better post-yield axial ductility due to their more substantial confinement effects [15]. Studies show that various factors affect the axial capacity of CFSTs, including the thickness of the steel tube, concrete strength, and the bond between the steel and concrete [16–19]. Additionally, the diameter of the steel tubes significantly influences the axial bearing capacity, with larger diameters potentially reducing the hoop stress and confinement effect [19,20].

Currently, the axial capacity of CFST columns is primarily calculated using existing design guidelines, including Eurocode 4 [21],

* Corresponding author.
E-mail addresses: dadelai@fafu.edu.cn (D. Lai), jingyu1.22@intl.zju.edu.cn (J. Wei), alessandro@fzu.edu.cn (A. Contento), junqing.xue@fzu.edu.cn (J. Xue), bruno@fzu.edu.cn (B. Briseghella), tommaso.albanesi@uniroma3.it (T. Albanesi), cristoforo.demartino@me.com (C. Demartino).

https://doi.org/10.1016/j.istruc.2024.107543
Received 26 July 2024; Received in revised form 7 October 2024; Accepted 10 October 2024
Available online 28 October 2024

Australia Standard/New Zealand Standard 2327 (AS/NZS2327) [22], and the American Institute of Steel Construction (ANSI/AISC 360-22) [23]. Additionally, several researchers have proposed feasible models for predicting the axial compressive load-carrying capacity of CFST columns (e.g., [17–19,24–29]). These models and specifications generally divide the axial compressive capacity of CFST into two contributing components: the internal concrete and the external steel tube. They account for the confinement effect provided by the outer steel tube on the core concrete, as well as differences in cross-sectional types.

However, the practicality of these models and guidelines is limited when dealing with conventional strength levels of inner concrete, cross-section dimensions, thickness, and the yield strength of the steel tube. For example, Eurocode 4 [21] is applicable only when the yield stress of the steel is within 460 MPa and the strength of the inner concrete is within 60 MPa. Similar material limitations are present in other code provisions.

In recent times, modern construction projects in building and infrastructure have increasingly embraced CFST columns with higher strength and larger cross-sections [30–32]. The use of materials such as High Strength Concrete (HSC), Ultra-High Performance Concrete (UHPC), and High Strength Steel Tubes (HSST) has gained significant attention due to their superior performance compared to conventional concrete and steel tubes. These CFST columns exhibit material properties and geometric characteristics that exceed the scope of current design codes.

Alternatively, Machine Learning (ML) models have recently been extensively applied in Civil Engineering to address complex problems that are challenging to solve with traditional methods [33,34]. A significant advantage of ML methods is that they do not require an extensive understanding of physical principles, thus lowering the application barrier for engineers. This makes ML models particularly suitable for guiding CFST design.

ML models offer significant potential for achieving enhanced accuracy in both regression and classification tasks compared to conventional methods such as physical tests, numerical simulations, and other data-driven approaches (e.g., [35–39]). In recent years, Machine Learning (ML) models have been successfully introduced and applied to predict the axial compressive capacity of CFST columns. Among these, the Artificial Neural Network (ANN) stands out as one of the most frequently adopted algorithms. For instance, Ahmadi et al. [40,41] trained ANN models to predict the axial compressive capacity of circular CFST columns using the Tansig-Linear activation function. Their results indicate that ANN models provide significantly more accurate and robust predictions compared to five traditional models.

Similarly, Tran et al. [42] developed a graphical user interface (GUI) tool for predicting the axial compressive capacity of circular CFST columns. Du et al. [43] created an ANN model for predicting the axial compressive capacity of rectangular CFST columns, utilizing data from 305 test results for stub rectangular CFST columns. In another study, Tran et al. [44] collected over 300 axial load test results for square CFST columns to train an ANN model. Additionally, Zarringol et al. [45] developed an ANN model that considers both rectangular and circular CFST sections. Their findings demonstrate that ANN models offer superior predictive performance and generalization capacity compared to traditional code methods.

Support Vector Machines (SVM) is another ML algorithm applied to predict the axial compressive capacity of CFST columns. Ngo et al. [46,47] utilized the SVM algorithm combined with grey wolf optimization to predict the axial bearing capacities of circular CFST columns. Similarly, Lyu et al. [48] developed an SVM model optimized by a sine cosine algorithm, achieving superior prediction performance compared to traditional design formulae.

In addition, the Adaptive-Network-Based Fuzzy Inference System (ANFIS) has gained significant favor for predicting the axial compressive capacity of CFST columns. This is evidenced by studies conducted by Tran and Kim [49], Le and Phan [50] and Zhou et al. [51]. More recently, Gradient Boosting Machine (GBM) algorithms have been increasingly adopted in structural engineering due to their higher prediction performance and efficiency. Vu et al. [52] developed an ML model based on the gradient tree boosting algorithm, while Lee et al. [53] trained a Category Boosting Algorithm (CatBoost) ML model to predict the axial compressive capacity of CFST columns. Both studies indicate that boosting algorithms offer higher training efficiency and superior predictive performance compared to other ML algorithms.

However, it is important to note that the aforementioned ML algorithms have largely overlooked the inherent uncertainty present in the input data. This uncertainty can arise from factors such as measurement errors or inadvertent discrepancies, highlighting the need for mitigation strategies to ensure the robustness and reliability of ML models. Such errors can lead to significant variability in the predicted axial compressive strength of CFST columns. Therefore, incorporating uncertainties into ML prediction models is crucial. Most traditional ML models, which provide only scalar predictions without uncertainty estimates, are inadequate for the probabilistic frameworks required in performance-based design [54]. To address these limitations, prior research has focused on integrating uncertainty into conventional models. For example, Bayesian-based models [55] and the Markov-Chain Monte Carlo (MCMC) method [56] have been used in predictive model development. More recently, a novel ML algorithm called Natural Gradient Boosting (NGBoost) has been proposed by Duan et al. [57]. NGBoost incorporates uncertainty estimation and has been successfully applied to predict structural behaviors (e.g., [58,59]). This approach allows for more reliable predictions by providing a measure of uncertainty alongside the point estimates.

While traditional ML models have shown significant promise in predicting the axial compressive capacity of CFST columns, they often fail to account for the inherent uncertainties in the input data, such as measurement errors and material inconsistencies. This lack of uncertainty quantification can lead to less reliable predictions, which is a critical limitation for performance-based design applications. Additionally, existing design codes and models are often constrained by material and geometrical limitations, making them inadequate for modern CFST applications that utilize high-strength materials and larger cross-sections. To address these gaps, this study introduces a probabilistic machine learning approach using Natural Gradient Boosting (NGBoost) to predict the axial compressive capacity of CFST columns. By leveraging a comprehensive dataset of 1127 experimentally tested CFST specimens and employing SHapley Additive exPlanations (SHAP) for feature importance analysis, the study demonstrates that the NGBoost model provides superior predictive accuracy and robustness. The performance of the model is benchmarked against existing design codes, showcasing its enhanced reliability and applicability for contemporary engineering challenges.

Following this introduction, this paper is organized as follows. Section 2 introduces the adopted database, which comprises a comprehensive collection of 1127 experimentally tested specimens of circular CFST columns subjected to axial compressive loads. Section 3 provides an overview of the adopted ML algorithms and the performance evaluation metrics. A probabilistic machine learning model (NGBoost) is formulated to achieve both high accuracy and probabilistic predictions, utilizing Normal and LogNormal distributions for predicting the targets (Section 3.2.2). Two deterministic ML models, eXtreme Gradient Boosting (XGBoost) [60], Artificial Neural Networks (ANN) [61], and another probabilistic ML model, XGBoost-Distribution (XGBD) [62], are also introduced to estimate the developed NGBoost predicted model. Section 4 presents the point and probabilistic prediction results. Section 5 provides discussions on ML model interpretation (Section 5.1.1), a parametric study (Section 5.2), and a comparison of performance with existing code provisions and predictive models (Section 5.3). Finally, in Section 6, the present study culminates with the synthesis of key findings and the exploration of future perspectives.

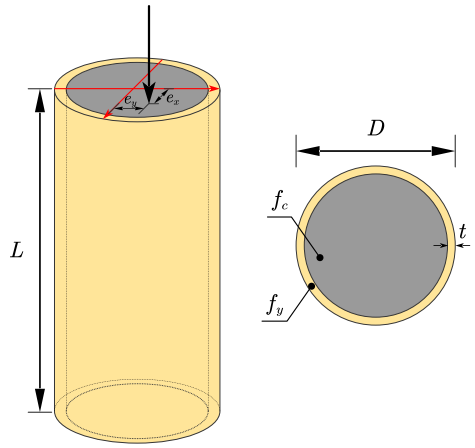

Fig. 1. Schematic diagram of a CFST column under axial compression, illustrating the defined input variables.

2. Database

In this section, we compiled a comprehensive database consisting total 1127 data points by gathering the experimentally test axial compressive capacity of CFST. CFSTs are composite structures combining the strength of steel and concrete to achieve high performance in construction. These tubes consist of a steel outer shell filled with concrete, leveraging the steel's tensile strength and concrete's compressive strength. The steel tube provides confinement to the concrete, enhancing its load-bearing capacity and preventing buckling, which leads to improved axial capacity and ductility.

Fig. 1 shows the schematic of a CFST column under axial compression and the definition of input variables. The input features are the diameter of the CFST column (D), thickness of the steel tube (t), the length of CFST column (L), the load eccentricity (e taken as the maximum of e_x and e_y), the compressive strength of inner concrete (f_c), and the yield strength of outer steel tube (f_y). The target label of the database is the axial compressive load capacity of CFST column (N_u). This extensive dataset serves as the foundation for developing and validating predictive models to accurately estimate the axial compressive capacity of CFST columns.

Table 1 presents the statistical description of all processed input features. Furthermore, Fig. A.17 in Appendix A displays a pair plot matrix representing all six input features and the target label. The database for this study comprises 1127 experimentally tested CFST specimens, providing a robust foundation for predicting axial compressive capacity. Key input features include the diameter of the CFST column (ranging from 25.40 mm to 1020.00 mm), the thickness of the steel tube (0.52 mm to 16.72 mm), the length of the CFST column (152.34 mm to 5400.00 mm), load eccentricity (0.00 mm to 300.00 mm), compressive strength of the inner concrete (9.16 MPa to 186.00 MPa), and yield strength of the outer steel tube (172.36 MPa to 1153.00 MPa). The target variable, axial compressive load capacity, spans from 14.41 to 46,000.00 kN. The standard deviation (SD) and coefficient of variation (CoV) for these variables indicate the variability within the dataset, ensuring a comprehensive representation of CFST column behaviors under axial loads. This extensive dataset allows for the development and validation of accurate and reliable ML models for predicting the axial compressive capacity of CFST columns.

3. Machine learning algorithms and performance metrics

This study aims to develop a comprehensive machine learning (ML) model capable of providing both accurate and probabilistic predictions of the axial compressive capacity of CFST columns. We introduced a probability-based ML algorithm, Natural Gradient Boosting (NGBoost) [57], to achieve high accuracy and incorporate uncertainty in the predictions. To better assess the prediction performance of developed NGBoost model, we also trained two widely adopted deterministic ML algorithms, XGBoost [60] and ANN [63], as well as another probability-based ML algorithm, XGBoost-Distribution (XGBD) [62] to serve as control groups.

Table 1
Summary of the database statistics for the axial compressive capacity of CFST. SD represents the standard deviation and CoV denotes the coefficient of variation.

Variables	Unit	Minimum	Maximum	Mean	Median	SD	CoV
D	[mm]	25.40	1020.00	157.51	139.70	90.80	0.57
t	[mm]	0.52	16.72	4.36	4.00	2.47	0.56
f_y	[MPa]	172.36	1153.00	351.99	328.00	112.96	0.32
f_c	[MPa]	9.16	186.00	52.04	41.57	29.60	0.56
L	[mm]	152.34	5400.00	1313.73	938.00	1051.04	0.80
e	[mm]	0.00	300.00	11.54	0.00	27.69	2.39
N_u	[kN]	14.41	46 000.00	1993.99	1022.00	3556.46	1.78

Fig. 2 illustrates the general schematic of the model development procedures, which include three main steps: data processing, model development, and model prediction. During the data processing step, the raw data was shuffled and split into a training set (75%) and a testing set (25%). In the model development step, the training set was used to train the selected ML algorithms. For NGBoost, XGBoost, and XGBoost-Distribution (XGBD), hyperparameters were optimized using a universal optimizer named BayesianOptimization API from the *bayes_opt* Python package [64]. The ANN model was constructed in Keras [65] and optimized using the ADAM optimizer [66].

All the developed ML models were validated utilizing the Mean Square Error (MSE) loss function, which evaluates the difference between the testing set and model predictions during the optimization iteration. The MSE is calculated as follows:

$$\mathrm{MSE} = \frac{1}{m}\sum_{i=1}^{m}\left(y_i - \hat{y}_i\right)^2 \tag{1}$$

where y_i and $\hat{y}_i$ represent the measured and predicted values of the target variable, respectively, for the i-th data point, and m is the total number of the data points.

The performance of the developed models was estimated using the testing set. The trained models were assessed using multiple performance metrics, including Root Mean Square Error (RMSE), Mean Absolute Error (MAE), Mean Absolute Percentage Error (MAPE), Median Absolute Error (MedAE), and the coefficient of determination (R^2), where $\bar{y}_i$ denotes the mean value of the predictions:

$$\mathrm{RMSE} = \sqrt{\frac{1}{m}\sum_{i=1}^{m}\left(y_i - \hat{y}_i\right)^2} \tag{2a}$$

$$\mathrm{MAE} = \frac{1}{m}\sum_{i=1}^{m}\mid y_i - \hat{y}_i \mid \tag{2b}$$

$$\mathrm{MedAE} = \mathrm{median}\left(\mid y_1 - \hat{y}_1 \mid, \mid y_2 - \hat{y}_2 \mid, \ldots, \mid y - \hat{y}_m \mid\right) \tag{2c}$$

$$\mathrm{MAPE} = \frac{100\%}{m}\sum_{i=1}^{m}\frac{\mid y_i - \hat{y}_i \mid}{y_i} \tag{2d}$$

$$\mathrm{R}^2 = 1 - \frac{\sum_{i=1}^{m}(\hat{y}_i - \hat{y}_i)^2}{\sum_{i=1}^{m}(y_i - \bar{y}_i)^2} \tag{2e}$$

3.1. Deterministic ML models

3.1.1. eXtreme Gradient Boosting (XGBoost)

eXtreme Gradient Boosting (XGBoost), initially introduced by Chen and Guestrin [60], is a gradient boosting algorithm that utilizes decision trees as base learners. One of its primary strengths is its scalability, making it well-suited for a wide range of scenarios. During the tree-growing process, XGBoost employs an exact greedy algorithm to determine the optimal splits, ensuring high efficiency in model development.

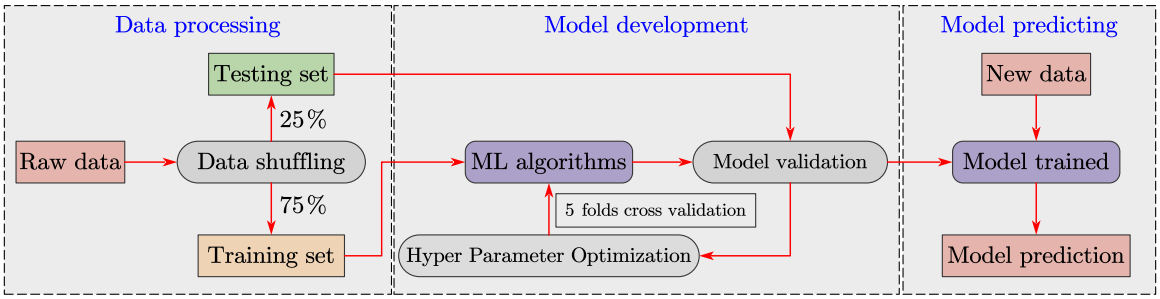

Fig. 2. Schematic representation of the model development process for each algorithm.

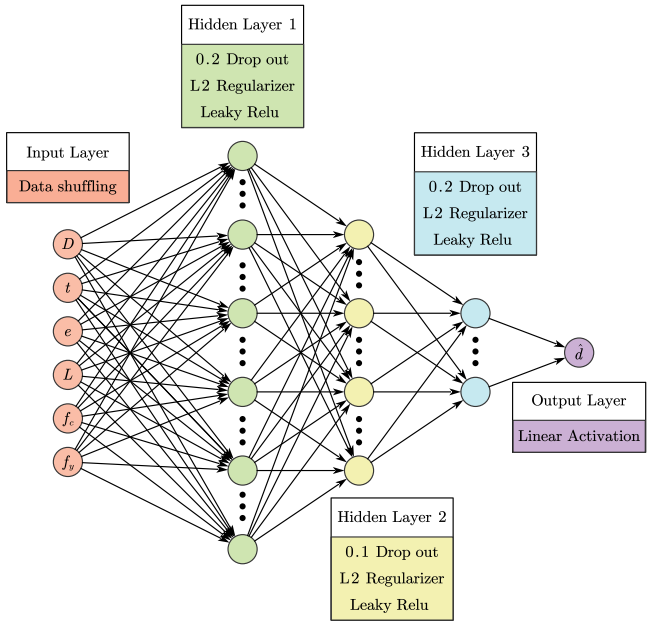

Fig. 3. Architectural configuration of the employed Artificial Neural Network (ANN) model.

Additionally, XGBoost adopts a systematic and iterative approach to building the ensemble model by sequentially adding weak learners that focus on samples with higher prediction errors. This iterative process allows the model to continually improve its predictive capability, leading to more accurate predictions. XGBoost leverages continuous scores (w_i) for each leaf in the decision trees, enhancing precision and adaptability. This approach ultimately results in an overall improvement in model performance.

3.1.2. *Artificial Neural Networks* (ANN)

Artificial Neural Networks (ANNs) are computational models inspired by the structure and functioning of the human brain [61]. They consist of interconnected nodes, known as "neurons", that process and transmit information. In this study, we adopted an ANN architecture similar to that proposed by Lai et al. [67], which includes an input layer, three hidden layers, and an output layer, as shown in Fig. 3. The input layer is a dense layer with 6 input features, while the three hidden layers consist of 128, 64, and 32 neurons, respectively. To counter overfitting and enhance the model's generalization ability, we introduced dropout layers with rates of 0.2 and 0.1 after each hidden layer, along with an L2 regularizer with a value of $\lambda = 0.01$. Leaky Rectified Linear Unit (ReLU) activation function [68] is employed to convert linear inputs into non-linear outputs.

3.2. *Probabilistic ML models*

3.2.1. *Xgboost-Distribution* (XGBD)

XGBoost Distribution (XGBD) is a Python-based API for machine learning probabilities developed by Donnerer [62]. It enables probabilistic predictions using the XGBoost framework by following a method similar to that demonstrated in the NGBoost library, which utilizes natural gradients to estimate distribution parameters. XGBD is designed to be compatible with the XGBoost scikit-learn API, with an additional keyword argument to specify the distribution type, making it highly flexible and user-friendly.

XGBD supports a variety of probabilistic distributions, including normal, LogNormal, and Poisson. This allows for a more comprehensive modeling of uncertainties in the prediction outcomes. The distributions are fitted using Maximum Likelihood Estimation (MLE), ensuring robust and reliable parameter estimation. The Normal distribution, denoted as $\mathcal{N}(\mu, \sigma^2)$, is a bell-shaped curve with parameters μ (mean) and σ (standard deviation). The LogNormal distribution, denoted as $LN(\mu, \sigma^2)$, is characterized by its logarithm following a Normal distribution. In the Normal distribution, the mean (μ) represents the central tendency of the distribution, while the standard deviation (σ) measures its dispersion. In the LogNormal distribution, the mean (μ) denotes the mean of the underlying Normal distribution on a logarithmic scale, and the standard deviation (σ) determines the spread of the LogNormal distribution on a logarithmic scale. In the case of a LogNormal distribution, the codomain is limited to positive real numbers, excluding zero. The Poisson distribution is used for modeling count data.

One of the key advantages of XGBD is its reported efficiency in providing probabilistic predictions compared to other methods, such as NGBoost [62]. This efficiency stems from its integration with the XGBoost framework, known for its high performance and scalability. XGBD leverages the exact greedy algorithm of XGBoost for determining optimal splits during the tree-growing process, which contributes to its high computational efficiency. Furthermore, XGBD maintains the iterative approach of XGBoost, where weak learners are sequentially added to focus on samples with higher prediction errors. This approach helps in continually refining the predictive model, leading to more accurate and reliable probabilistic predictions. By allowing the specification of different distributions, XGBD provides the flexibility to tailor the model to the specific characteristics of the data, thereby enhancing its applicability across various domains.

3.2.2. *Natural Gradient Boosting* (NGBoost)

NGBoost, introduced by Duan et al. [57], is a probabilistic machine learning algorithm known as Natural Gradient Boosting. Its primary aim is to provide accurate predictions while also estimating uncertainty. NGBoost follows a boosting methodology similar to traditional gradient boosting algorithms but distinguishes itself by focusing on modeling the conditional distribution of the output given the input variables. By integrating probabilistic modeling techniques, NGBoost can offer a measure of uncertainty in its predictions, setting it apart from deterministic boosting algorithms that focus solely on point estimates.

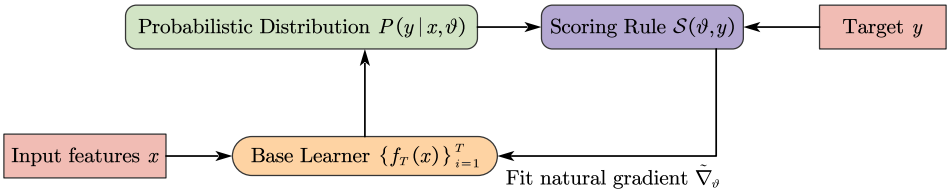

Fig. 4. Schematic diagram of the NGBoost algorithm, adapted from Duan et al. [57].

Table 2
Performance metrics (see Eq. (2)) of the 6 ML models for the training set, testing set, and full dataset. The training time is given in seconds. The basic units of the performance metrics are the same as those for y_i and $\hat{y}_i$, i.e., kN.

Model	Training time	Training set					Testing set					Full dataset				
		RMSE	MAE	MAPE	MedAE	R^2	RMSE	MAE	MAPE	MedAE	R^2	RMSE	MAE	MAPE	MedAE	R^2
XGBoost	1.55	347.04	47.98	0.0196	6.61	0.9902	348.41	149.47	0.2372	56.62	0.9902	347.38	73.38	0.0740	11.28	0.9902
ANN	260.78	302.60	161.41	0.1283	88.02	0.9920	397.19	202.26	0.1636	110.66	0.9868	328.83	171.63	0.1371	94.48	0.9907
XGBD- $\mathcal{N}(\mu, \sigma^2)$	1.89	168.22	105.65	0.1025	70.81	0.9977	876.74	263.54	0.1848	114.54	0.9509	462.12	145.16	0.1231	79.01	0.9839
XGBD- L$\mathcal{N}(\mu, \sigma^2)$	2.11	338.17	95.97	0.0583	44.43	0.9901	570.64	205.93	0.1173	83.22	0.9748	408.93	123.49	0.0730	47.67	0.9860
NGBoost - $\mathcal{N}(\mu, \sigma^2)$	6.70	400.25	123.69	0.0895	61.70	0.9868	447.13	200.46	0.1381	94.24	0.9828	412.48	142.90	0.1017	68.30	0.9858
NGBoost - L$\mathcal{N}(\mu, \sigma^2)$	8.85	223.52	69.14	0.0420	29.78	0.9959	310.29	144.25	0.0965	65.65	0.9919	248.09	87.93	0.0557	34.62	0.9949

Fig. 4 illustrates the schematic diagram of the fundamental modeling process for the NGBoost algorithm. Initially, the input data x is trained by the base learners. Unlike deterministic boosting ML algorithms where the output y given input data x is a scalar value, NGBoost models the output as a conditional distribution $P(y \mid x, \vartheta)$. The parameters ϑ are the parameters of the probabilistic distribution used to model the target variable. In the NGBoost algorithm, various probabilistic distributions can be adopted during the model development step based on the input variable structures to achieve improved prediction performance. NGBoost supports various distributions, including Normal and LogNormal. The parameters ϑ are determined using conventional gradient boosting techniques. This approach allows NGBoost to capture the uncertainty in the predictions by providing a distribution rather than a single value.

Implementing the loss function in conventional gradient boosting algorithms poses challenges when applied to multidimensional prediction tasks involving parameters such as μ and σ. Therefore, NGBoost adopted a scoring rule, $\mathcal{S}(\vartheta, y)$, to evaluate the forecast's quality. The suggested scoring rules are the Maximum-Likelihood Estimation (MLE) and the Continuous Ranked Probability Score (CRPS) [57,58]. To accommodate multidimensional prediction results and mitigate the influence of probability distribution parameterization, the natural gradient is chosen instead of the numerical gradient for training the new base model, $f_K(x)$. The inclusion of the natural gradient in the training process considers the intrinsic characteristics of the parameter space, facilitating more optimal and robust updates.

4. Results

4.1. Point prediction

Point prediction refers to the process of estimating a single, specific value as the output of a predictive model. In the context of machine learning and statistical modeling, point predictions are the direct output values generated by the model for a given set of input variables. While deterministic models provide a single point prediction, probabilistic models generate a distribution of possible outcomes, and this will be discussed in Section 4.2.

Table 2 summarizes five performance metrics, as defined in Eq. (2), that quantitatively assess the accuracy of the ML model predictions compared to the corresponding experimental data. Additionally, the table presents the computational time (in seconds) required for training the various models. It is observed that among the two deterministic ML models, XGBoost and ANN, XGBoost consistently yields more accurate predictions, particularly for the training set. Furthermore, XGBoost demonstrates a significant advantage in terms of model training efficiency compared to ANN. The XGBD probabilistic ML models, utilizing both Normal and LogNormal distributions, show a slight decrease in prediction accuracy compared to the XGBoost deterministic model, especially for the testing set. Notably, the XGBD model with the LogNormal distribution exhibits superior performance on the testing set for mean predictions, indicating less over-fitting behavior. The NGBoost probabilistic models, employing both Normal and LogNormal distributions, demonstrate exceptional generalization and accuracy for the mean predictions, as evidenced by the closely matched predicted performance on both the training and testing sets. Similar to the XGBD models, the mean prediction performance of the NGBoost probabilistic model with the LogNormal distribution surpasses that with the Normal distribution in both the training and testing sets.

Comparatively, while the NGBoost models provide higher accuracy in mean predictions, they exhibit less efficiency in model training compared to the XGBD probabilistic models. This trade-off between prediction accuracy and training efficiency highlights the strengths and limitations of each model, providing valuable insights for selecting the appropriate ML model based on specific application requirements.

Fig. 5 presents a comparison between the measured and mean predicted axial compressive capacity of CFST columns using all six ML models. The inset subfigures provide a detailed view of the data scale, ranging from 0 to 10000 kN, a critical range of data intensity. Overall, across all six ML models, the data points are evenly distributed along the 1:1 line, with few outliers falling outside the ±20% bound, indicating a high level of prediction accuracy compared to the experimental data.

However, the XGBoost model's predictions exhibit more outliers, particularly in the testing set for axial compressive capacities within 10,000 kN. When examining the XGBD probabilistic model with a Normal distribution, its prediction performance closely resembles that of the XGBoost model, albeit with a few outliers in the testing set that overestimate the axial compressive capacity.

In contrast, the XGBD model with a LogNormal distribution shows less biased predictions within the 10000 kN range and fewer outliers when the capacity exceeds 10,000 kN. The NGBoost probabilistic models offer superior predictions compared to the XGBD models, evidenced by fewer outliers both within and beyond the 10,000 kN range. Notably, the NGBoost model with a LogNormal distribution demonstrates the best predictions among the six models, with almost all predictions falling within the ±20% bound.

Fig. 6 provides a comprehensive evaluation of all six developed ML models using Taylor diagrams. These diagrams offer a consolidated

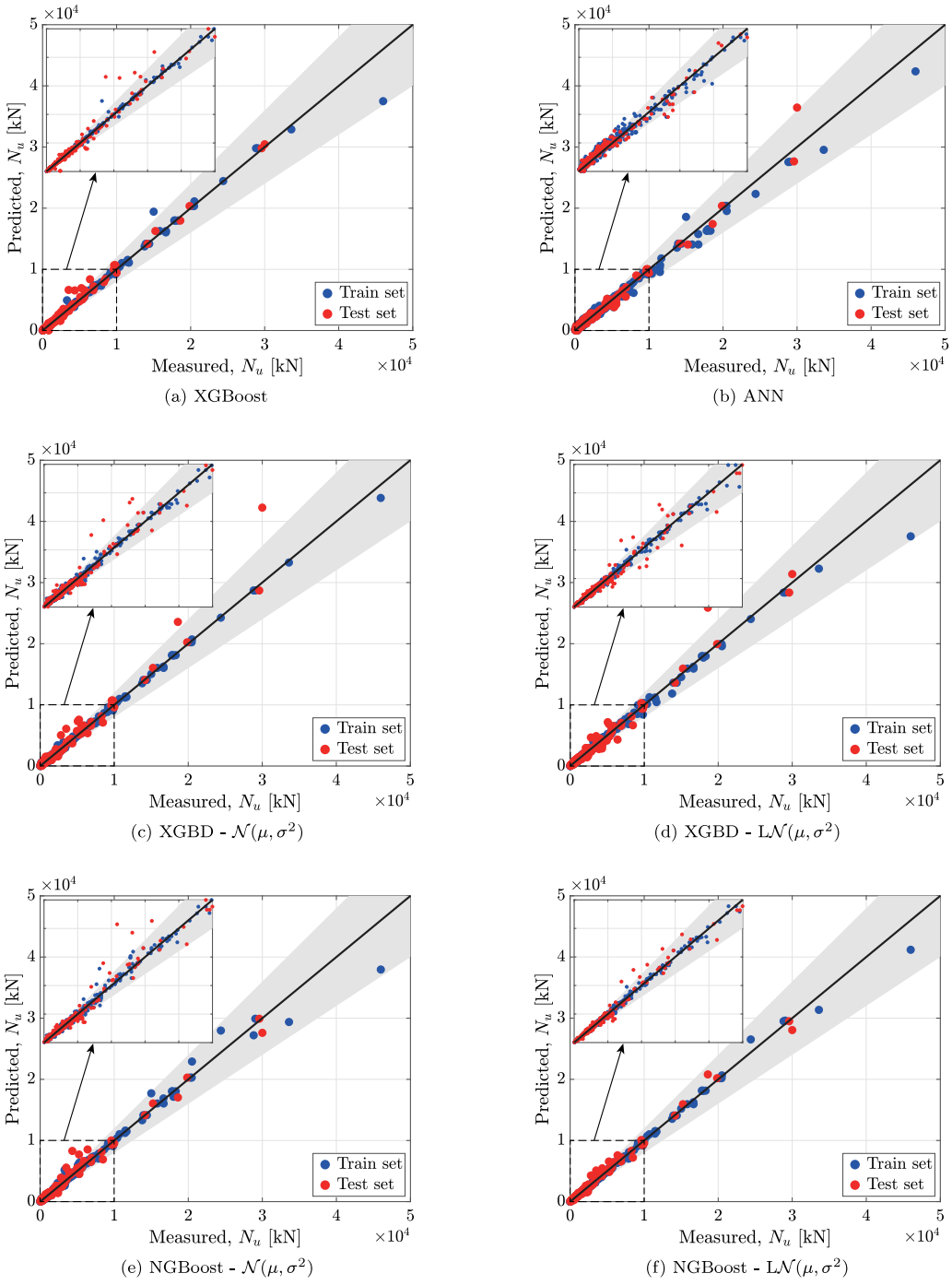

Fig. 5. Comparison between the measured and predicted axial compressive capacity of CFST columns, with a gray area indicating an error bound of ±20%. The inset subfigure provides a detailed view of the scale ranging from 0 to 10,000 kN, highlighting a critical range of data intensity.

representation of various aspects of model performance in a single plot, including the correlation coefficient (r), normalized standard deviations, and the distance from the observation point [69], which signifies the centered RMSE (see Eq. (2a)). The points representing observed values on the x-axis correspond to the measured experimental values and have a unit correlation coefficient, essentially representing a perfect model. The closer a predicted model is to these observed points, the better its performance.

It is evident that the XGBD model with a Normal distribution demonstrates the best performance on the training set, followed by the XGBD model with a LogNormal distribution and the NGBoost model with a LogNormal distribution. However, both XGBD probabilistic models exhibit poorer performance on the testing set, particularly concerning standard deviation. In contrast, the NGBoost model with a LogNormal distribution exhibits the best mean predictions among all ML models. This indicates its superior generalization ability and robustness in predicting the axial compressive capacity of CFST columns.

In conclusion, for point prediction, the NGBoost model with a LogNormal distribution yields superior accuracy among the six ML models. The two XGBD probabilistic models deliver excellent mean prediction results on the training set but exhibit considerably worse performance on the testing set, indicating potential over-fitting issues.

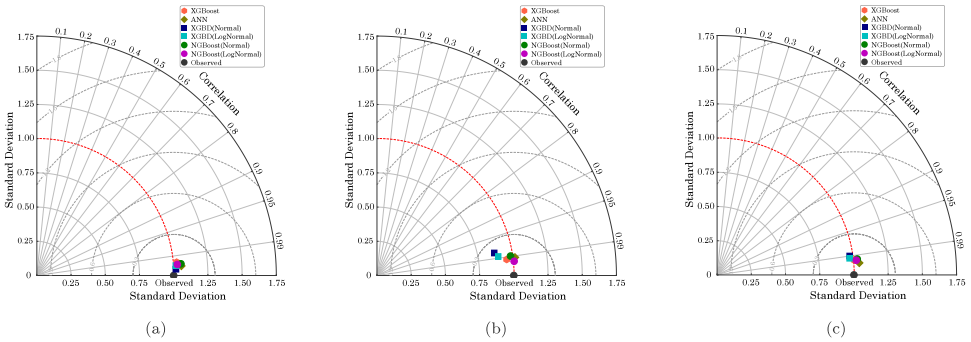

Fig. 6. Taylor diagram of the training (a), testing (b), and full dataset (c) of the ML models.

The deterministic XGBoost model shows similar prediction performance to the XGBD models.

4.2. Probabilistic predictions

Fig. 7 shows the probabilistic prediction results for the four probabilistic ML models. The solid gray line represents the mean predictions (μ) corresponding to the measured data, shown as red dots. The filled colors represent three confidence intervals: $\mu \pm \sigma$, $\mu \pm 2\sigma$, and $\mu \pm 3\sigma$ (σ being the standard deviation).

Fig. 7(a) shows the probabilistic predictions for XGBD with a Normal distribution. It is observed that almost all measured data points fall within the confidence interval of $\mu \pm \sigma$, indicating a prediction confidence of 68.2% when $N_u < 2000$ kN. However, more outliers fall outside this confidence interval when $N_u > 2000$ kN, suggesting that the model performs better for smaller axial compressive capacities compared to larger ones.

As shown in Fig. 7(b), For the XGBD model with a LogNormal distribution, the prediction performance aligns well with the measured actual data points when $N_u < 1000$ kN and $N_u > 10000$ kN, confirmed by the majority of red points falling within the $\mu \pm \sigma$ confidence interval. Notably, the confidence interval is significantly narrower (i.e., lower standard deviation) for $N_u < 3000$ kN in this model compared to the XGBD model with a Normal distribution, indicating higher prediction confidence for the axial compressive capacity of CFST in this range.

For the NGBoost model with a Normal distribution (see Fig. 7(c)), the confidence intervals are remarkably narrower compared to those of the XGBD model with a Normal distribution. This implies that the NGBoost model provides a higher level of prediction confidence than XGBD with a Normal distribution. Moreover, unlike the XGBD model, which maintains relatively constant standard deviations, the standard deviations for NGBoost model predictions with a Normal distribution vary significantly, resulting in a more pronounced and dynamic appearance of the confidence intervals. This suggests that the NGBoost model is more sensitive to each individual prediction.

Fig. 7(d) illustrates the case of NGBoost with a LogNormal distribution. Similar to NGBoost with a Normal distribution, this model exhibits significantly lower and more dynamically changing standard deviations compared to the XGBD model with a LogNormal distribution (XGBD - $\mathrm{L}\mathcal{N}(\mu, \sigma^2)$). Furthermore, in contrast to the NGBoost model with a Normal distribution, it showcases unbiased predictions across the entire range of axial compressive capacity predictions. Additionally, the confidence intervals are even narrower than those of the NGBoost model with a Normal distribution, indicating that this model provides the highest confidence in predicting the axial compressive capacity of CFST columns.

Fig. 8 shows the probability density functions (PDFs) for two selected cases in the two NGBoost models, along with the measured test data and the mean predictions of the other four models. The corresponding input features, experimental targets, and predictions of the six models for these two selected cases are summarized in Table 3. These cases are chosen from the database to represent relatively low and high axial compressive capacities of CFST columns. These cases will be referenced in subsequent sections of this study.

In the first case, it is evident that the confidence intervals of the LogNormal distribution are smaller than those of the Normal distribution, affirming the higher prediction confidence of NGBoost with a LogNormal distribution. However, the mean prediction from the Normal distribution is more accurate than that from the LogNormal distribution. Among the other ML models, the XGBoost model's prediction is almost identical to the actual value. In contrast, the ANN model tends to overestimate the axial compressive capacity, while the mean predictions of the two XGBD models tend to underestimate the capacity. In the second case, the predictions from the two NGBoost models are quite similar, with closely aligned mean predictions and confidence intervals. The XGBoost model slightly overestimates the capacity, while the other ML models tend to underestimate the outputs.

5. Discussion

5.1. Model interpretation

From Section 4, we concluded that the predictive performance of the NGBoost model with a LogNormal distribution surpasses that of other ML models in terms of both point and probabilistic prediction. Therefore, this section focuses solely on this model for further interpretation and analysis.

5.1.1. SHapley Additive exPlanations (SHAP)

The six aforementioned ML models demonstrate satisfactory accuracy and efficiency in predicting the axial compressive capacity of CFST columns. However, their inherent black-box nature limits their interpretability and practical application in solving real engineering problems. Fortunately, various model interpretation techniques have been developed to provide comprehensive explanations for ML models. These include Local Interpretable Model-Agnostic Explanations (LIME), Interpretable Mimic Learning (IML), and SHapley Additive exPlanations (SHAP). Among these interpreters, SHAP is the most widely adopted, as it not only offers global interpretation but also supports local explanations. Additionally, SHAP provides a powerful plot API, making it easier to visualize model interpretation results.

SHAP is inspired by cooperative game theory, quantifying the contribution of each input feature using SHapley values [70]. Considering a model prediction, $f(x)$, derived from a single input feature, x, the prediction can be expressed using an additive feature attribution method [70]:

$$f(x) = g\left(x'\right) = \phi_0 + \sum_{i=1}^{I} \phi_i x'_i \tag{3}$$

where x' is defined as a simplified input that is mapped to the original inputs through a mapping function, $x = h_x(x')$. The constant term, $\phi_0 = f\left(h_x(0)\right)$, represents the prediction when all inputs are null. The

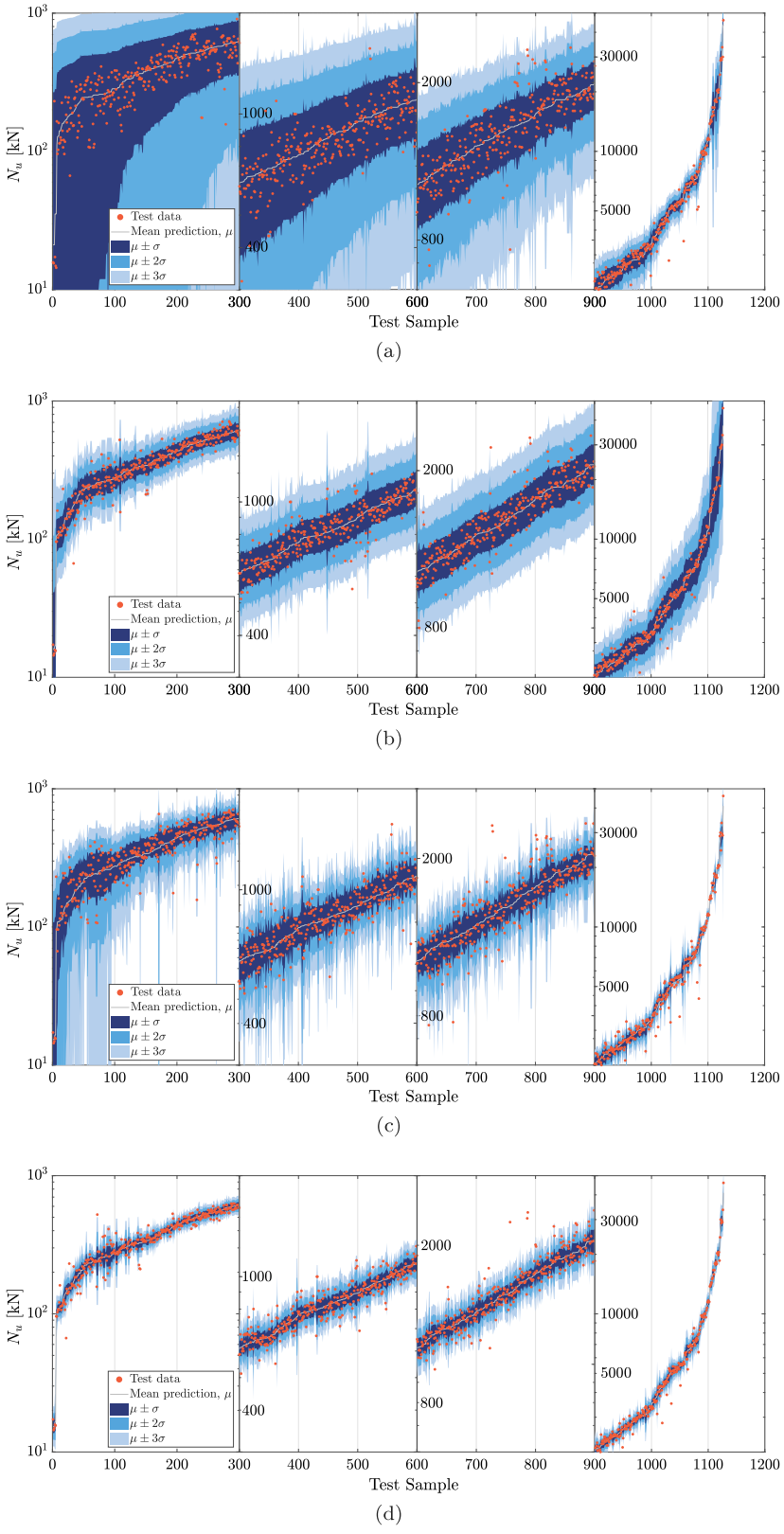

Fig. 7. Model prediction performances of (a) XGBD - $\mathcal{N}(\mu, \sigma^2)$, (b) XGBD - L$\mathcal{N}(\mu, \sigma^2)$, (c) NGBoost - $\mathcal{N}(\mu, \sigma^2)$, and (d) NGBoost - L$\mathcal{N}(\mu, \sigma^2)$. μ is the mean prediction. The filled colors represent three confidence intervals, i.e., $\mu \pm \sigma$, $\mu \pm 2\sigma$, and $\mu \pm 3\sigma$. Note the y-axes are different in each subfigure and are in log scale.

Table 3
Input features, experimental targets, and predictions of the six models for the two selected cases investigated. Note: all units of the input features are consistent with Table 1. For the four probabilistic models, the standard deviations are shown in brackets.

No.	D	t	f_c	f_y	L	e	N_u	NGBoost - $\mathcal{N}(\mu,\sigma^2)$	NGBoost - L$\mathcal{N}(\mu,\sigma^2)$	XGBoost	ANN	XGBD-$\mathcal{N}(\mu,\sigma^2)$	XGBD-L$\mathcal{N}(\mu,\sigma^2)$
1	102.7	1.65	40.9	265.1	309	0.00	485	473(60)	449(1.05)	485	520	426(246)	439(1.12)
2	559.4	16.54	31.7	546.0	995	0.00	29 590	29908(2243)	29506(1.06)	29 823	27 538	28708(3537)	28363(1.50)

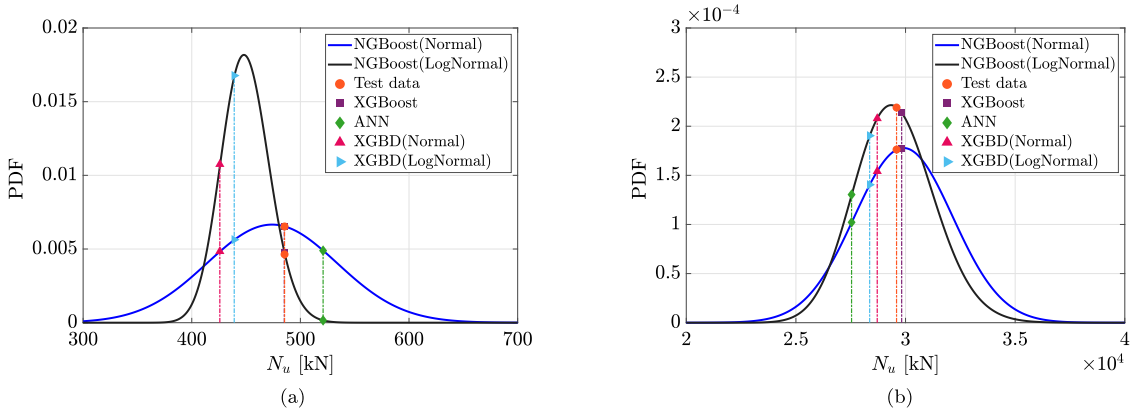

Fig. 8. Predicted probabilistic axial compressive capacity of two example cases (see Table 3) from NGBoost models with Normal ($\mathcal{N}(\mu,\sigma^2)$) and LogNormal (L$\mathcal{N}(\mu,\sigma^2)$) distributions compared with the corresponding measured values and mean predictions from XGBoost, ANN, and XGBD with $\mathcal{N}(\mu,\sigma^2)$ and L$\mathcal{N}(\mu,\sigma^2)$.

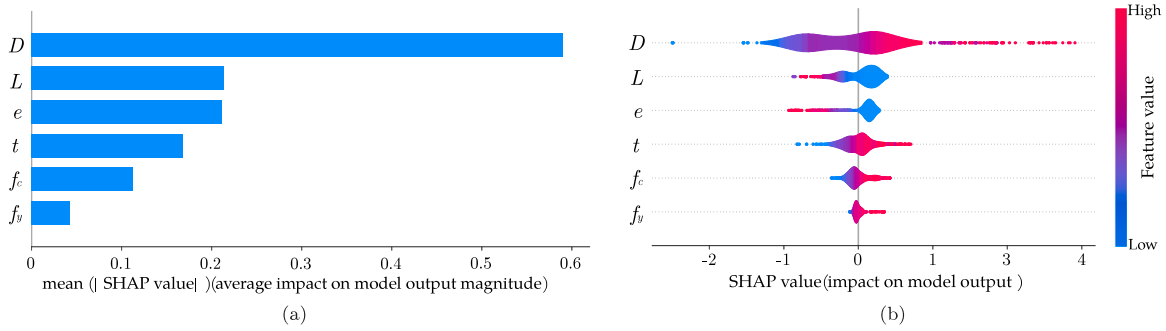

Fig. 9. Global interpretations of NGBoost model with LogNormal distribution by SHAP values: (a) SHAP feature importance and (b) SHAP summary plot.

attribution values for feature i are denoted as ϕ_i, and I represent the total number of features. By solving this equation, the SHAP values can be calculated, providing insights into the contribution of each feature to the model's predictions.

5.1.2. Global interpretation

In Fig. 9, the global interpretation results are presented, including both the feature importance and interpretation summary information. Analyzing the feature importance results, it becomes evident that the diameter of the CFST column (D) significantly governs the axial compressive capacity of CFST, indicating notably higher importance compared to other input features. Following closely are the length of the column (L) and the load eccentricity (e), which exhibit nearly equal influence on the model outputs after the diameter of the CFST column. The thickness of the steel tube (t) ranks as the fourth influential input feature, slightly less important than L and e. In comparison, the compressive strength of the inner concrete (f_c) holds more importance than the yield strength of the outer steel tube (f_y) in the model predictions, which is agree well with the finds from Contento et al. [18].

Fig. 9(b) is a SHAP summary plot that illustrates the impact of various features on the model's output using SHAP values. The x-axis represents the SHAP values, which indicate the impact of each feature on the model's prediction. The color gradient from blue to red indicates the feature values, with blue representing low feature values and red representing high feature values. The distribution of SHAP values for each feature is shown as a violin plot. Wider sections of the plot indicate a higher density of data points with similar SHAP values. Positive SHAP values on the left side of the vertical line indicate that increasing the feature value enhances the model prediction, whereas negative SHAP values on the right indicate that increasing the feature value diminishes the model prediction.

The SHAP summary plot clearly indicates that an increase in the diameter of the CFST column significantly enhances the axial compressive capacity of CFST. This suggests that the most effective approach to improve axial load resistance is by increasing the size of the CFST column. Conversely, both the length of the CFST column and the load eccentricity exhibit a negative relationship with the final outputs. This is understandable as increases in L and e tend to cause instability issues under axial compressive loads, thereby reducing the column's load-bearing capacity. The remaining input features, t, f_c, and f_y, positively influence the axial compressive load capacity of the CFST column. Overall, geometric parameters such as D, L, and t, are more critical in determining the axial compressive capacity of CFST columns than material-related parameters (f_c and f_y). This emphasizes the importance of focusing on geometric aspects rather than solely on material properties when designing axially loaded CFST columns.

In Fig. 10, feature dependence plots based on SHAP values are provided for all six input features, ordered by their feature importance (see Fig. 9(a)). These plots visually represent the relationship between specific features and their corresponding SHAP values, illustrating how

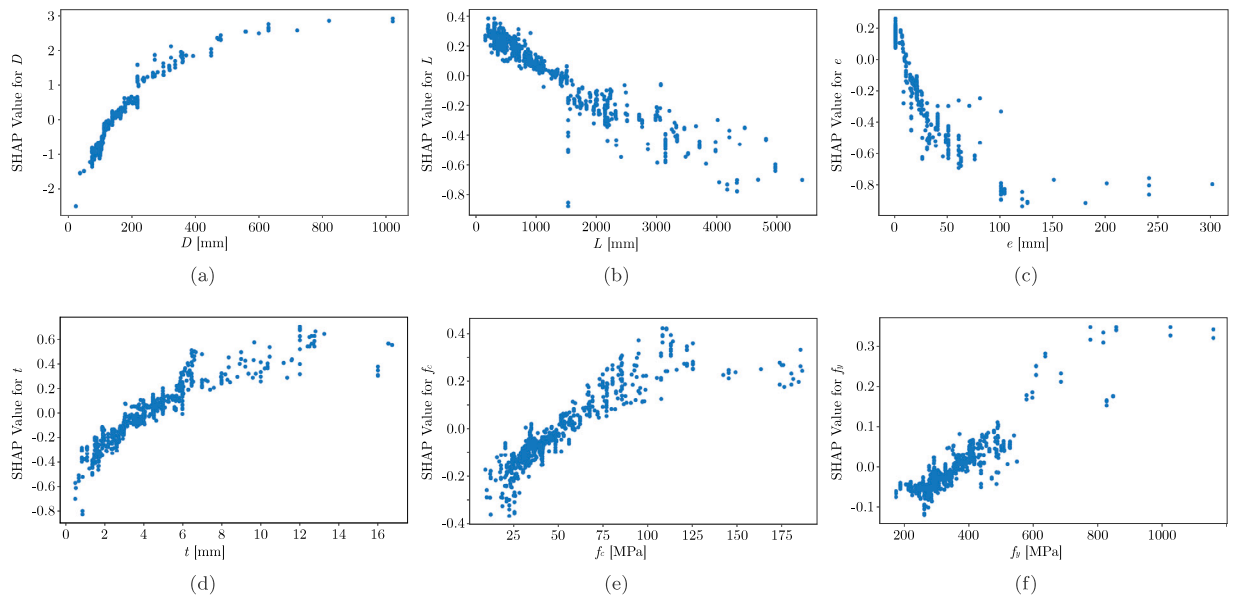

Fig. 10. Feature dependence plots by SHAP values for: (a) D; (b) L; (c) e; (d) t; (e) f_c; (f) f_y.

Fig. 11. Local interpretations of the NGBoost model with LogNormal distribution by SHAP values of two example cases (see Table 3): (a) case one and (b) case two.

each feature's value influences the model's predictions while controlling for other features. The y-axis represents the calculated SHAP values for each input feature, while the x-axis denotes the actual feature value for each data point in the database.

It is evident that features D, f_c, and f_y are positively related to the SHAP values, whereas an increase in features L and e tends to reduce the corresponding SHAP values. This agree well with the findings from the summary plot in Fig. 9(b). For the diameter of the CFST column, it is found that the SHAP value shows a linear increase with the diameter (D) when $D < 400$ mm. However, as the diameter further increases, the enhancement in SHAP value becomes less significant. This suggests that increasing the diameter of CFST is not as economically beneficial for enhancing axial compressive capacity when the diameter is greater than 400 mm.

Conversely, the feature L is almost linearly and negatively related to its SHAP value across the entire range of the database, indicating that it is possible to mitigate the loss of axial compressive capacity by controlling the length of the CFST column. For load eccentricity (e), the SHAP value significantly decreases as e increases from 0 to 100 mm, while further increases in e induce a less pronounced decrease in the SHAP value.

The trends of SHAP value for t and f_c are similar to the case of D. For t, with the majority thickness of the steel tube being less than 8 mm, the SHAP value nearly linearly increases with the increase of t when $t < 8$ mm, but the enhancement becomes less remarkable when t exceed 8 mm. In the case of f_y, it is observed that the majority of yield strengths of the steel tube fall between 200 to 400 MPa, and the increase in f_y is almost linearly related to the corresponding SHAP value.

5.1.3. Local interpretation

Fig. 11 provides a local interpretation from SHAP for two samples taken from the database represent the low and high axial compressive capacity of CFST (for detailed information, see Table 3). The tested capacities are 485 and 29590 kN, and the NGBoost model (with LogNormal distribution) predictions are 449 and 29506 kN, respectively. In each subfigure, the base value represents the mean value of the model predictions for the entire database. The x-axis denotes the model outputs from the base value, while the y-axis shows the influential input features ordered by their importance for the given case.

For the first sample (Fig. 11(a)), the most influential feature is the diameter of the CFST column, contributing −1145 kN to the axial compressive capacity, as its value is significantly less than the mean value of the database. Similarly, the following important feature, t, reduces the expected axial compressive capacity by about 443 kN, due to its relatively low thickness value. Other negatively influential features include f_c and f_y, contributing −115 kN and −83 kN to the

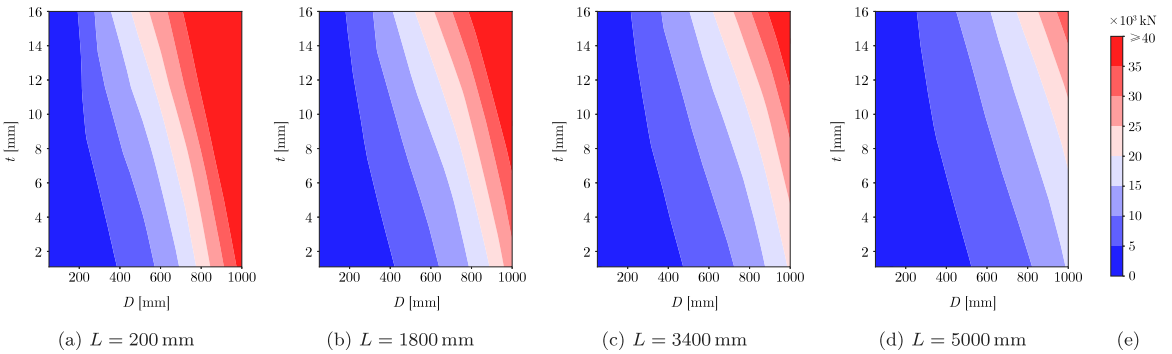

Fig. 12. NGBoost model with LogNormal distribution mean prediction response for L varied within the range of 200 to 5000 mm (a-d).

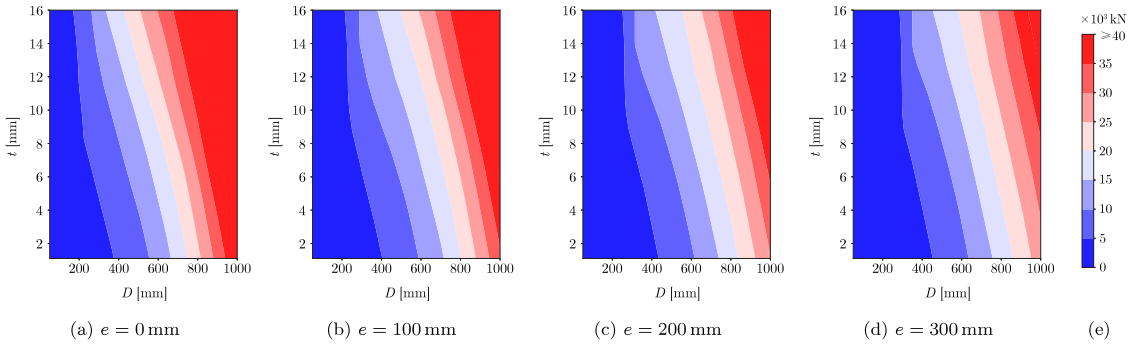

Fig. 13. NGBoost model with LogNormal distribution mean prediction response for e varied within the range of 0 to 300 mm (a-d).

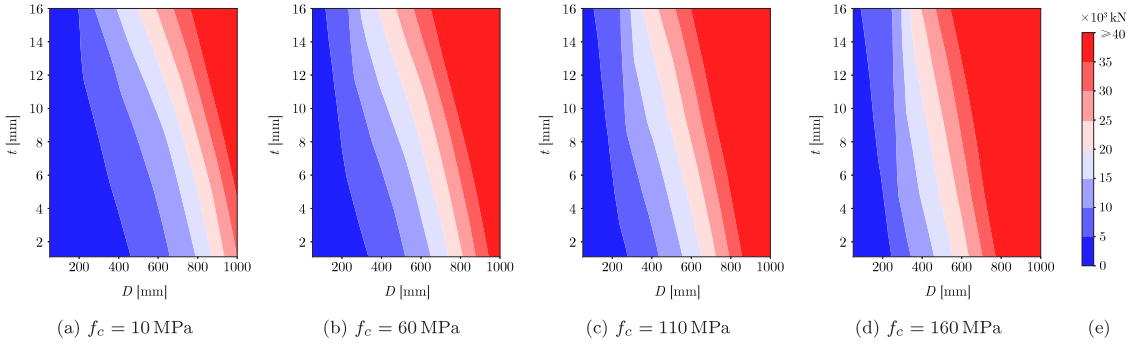

Fig. 14. NGBoost model with LogNormal distribution mean prediction response for f_c varied within the range of 10 to 160 MPa (a-d).

capacity, respectively. Conversely, the only two positively influential features in this case, L and e, tend to increase the capacity by 148 kN and 108 kN.

For the second case (Fig. 11(b)), the most influential features are D and t. Higher values of these two features tend to enhance the final axial compressive capacity prediction by about 19913 kN and 7899 kN. Compared to D and t, the remaining features show a negligible influence on the final prediction, each contributing less than ±400 kN.

5.2. Parametric study

A parametric study was conducted to further investigate insights from the developed NGBoost model with a LogNormal distribution and to facilitate practical applications. The following discussion focuses on a systematic analysis based on a specific pair of input features within defined ranges: the diameter of the CFST (D) ranging from 50 to 1000 mm and the thickness of the steel tube (t) ranging from 1 to 16 mm. Parameters D and t were chosen for analysis as they represent important cross-section properties and have been identified as two of the most significant geometric parameters related to the steel tube. Simultaneously, a third input feature was varied to its lowest and highest valid values (see Table 1), while the other features were kept constant at their respective median values (see Table 1). The parametric results are illustrated using contour plots, where the x and y axes represent the varying CFST diameter (D) and the steel tube thickness (t), while different colors denote the model predictions.

Fig. 12 shows the model predictions for four different CFST column lengths (L), which align well with the observed trend of decreasing capacity predictions as L increases. In each subfigure, it is observable that the diameter (D) exhibits a more pronounced influence on the model predictions than the thickness of the steel tube (t). When $D <$ 200 mm, the model predictions are consistently less than 5000 kN regardless of high values of t and small values of L.

Fig. 13 demonstrates the model predictions for different load eccentricities (e). Similar to the case of L, an increase in e effectively reduces the model prediction. Moreover, the decrease in model prediction from e = 0 to 100 mm is more pronounced than the decrease in model prediction from e = 100 to 300 mm, which agrees with the results shown in Fig. 10(c). Figs. 14 and 15 present the model predictions according to different strengths of inner concrete and outer steel tube.

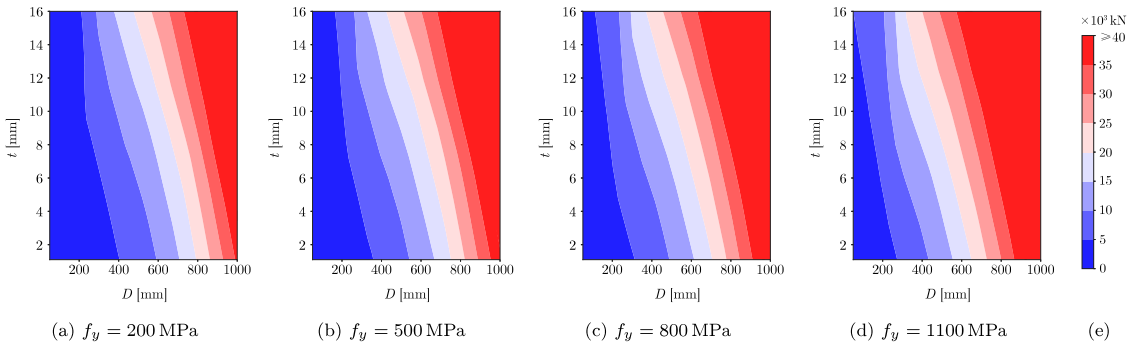

Fig. 15. NGBoost model with LogNormal distribution mean prediction response for f_y varied within the range of 200 to 1100 MPa (a-d).

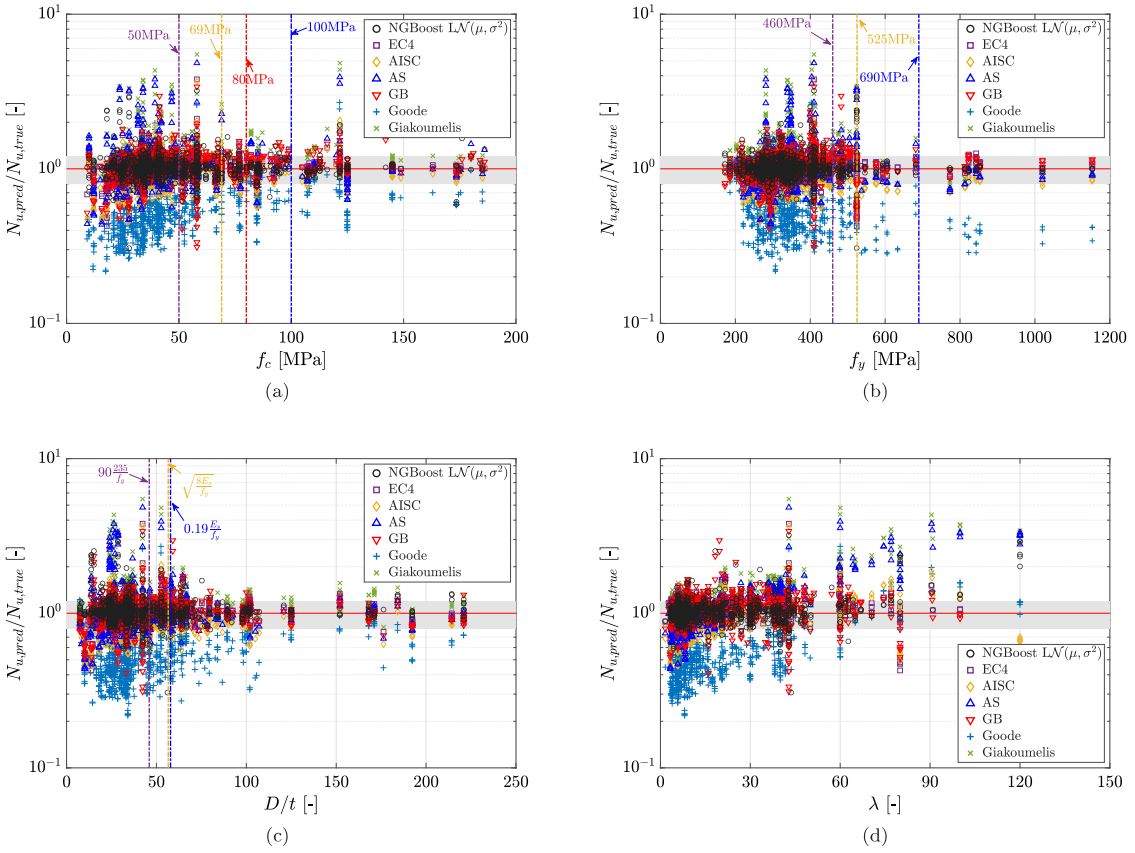

Fig. 16. Comparison of performance with existing code provisions and predictive models with respective to (a) f_c, (b) f_y, (c) D/t, and (d) λ. The gray area indicates an error bound of ±20%.

The increasing trend in model predictions with the increase in material strength is consistent across both parameters. However, due to the more significant influence of f_c than f_y, the increase in model predictions is more pronounced when f_c = 10 to 160 MPa than when the yield strength of the steel tube changes from f_y = 200 to 1100 MPa.

5.3. Evaluation of predictive performance: NGBoost vs. Existing code provisions and models

This section aims to introduce widely used standard code provisions and models for determining the axial compressive load capacity of CFST columns. A comparison of the predictive performance between the existing provisions, models, and the developed NGBoost model with a LogNormal distribution is presented to provide a comprehensive assessment of the proposed ML model for real design applications. The discussed code standards include the European Code 4 (EC4) [21], the American Institute of Steel Construction (ANSI/AISC 360-22) [23], the Australia Standard/New Zealand Standard (AS/NZS 2327) [22] and Chinese national CFST standard [71]. Additionally, two theoretical models proposed by Goode and Narayanan [24] and Giakoumelis and Lam [25] are taken into consideration for this comparison. A review of these models is provided in Appendix B. This analysis aims to evaluate the accuracy and applicability of the NGBoost model in real-world design scenarios.

Fig. 16 illustrates a performance comparison between the developed NGBoost model with LogNormal distribution and existing code provisions and predictive models concerning f_c, f_y, D/t, and λ (slenderness ratio for an RC column, which is equal to kL/r, with r representing the radius of gyration of its cross-section; k denotes a constant reflecting the end conditions of the column). The first three variables are displayed on the x-axis to enable a thorough comparison of predictive

performance, both within and beyond the limitations of the existing code provisions. The slenderness ratio, λ, is employed to evaluate the model's performance for CFST columns with varying slenderness ratios. The y-axis represents the ratio of predicted values to the actual true values. It is important to note that only data without eccentric load were considered for the existing code provisions and predictive models, as most of these models do not account for load eccentricity. Table 4 lists the comparison of the performance metrics (see Eq. (2)) results between the proposed NGBoost - L$\mathcal{N}(\mu, \sigma^2)$ model and the four code based models as well as two existing computation models for the axial compressive capacity of CFST column.

Fig. 16(a) illustrates a comparison with respect to f_c. For the developed NGBoost model with a LogNormal distribution, the majority of data points fall within the ±20% error bound, indicating precise predictions. The outliers are mostly in the range when $f_c < 60$ MPa, resulting from overestimation of the axial compressive capacity of CFST columns. Conversely, for higher f_c values, the NGBoost model exhibits excellent prediction performance in terms of accuracy.

Regarding the EC4 code provisions, their application is limited to $f_c \leq 50$ MPa. However, the prediction performance for EC4 when $f_c > 50$ MPa is generally better than within the 50 MPa, where the provisions tend to underestimate the axial capacity, especially for f_c lower than 30 MPa. The prediction performance of the AISC provisions is similar to that of EC4, characterized by evident underestimations of axial compressive capacity when f_c is lower than 50 MPa, while providing generally better predictions for higher f_c.

The prediction outcomes from AS2327 show less biased behavior, with both overestimated and underestimated outliers observed. The prediction from Chinese GB50936-2014 code exhibits acceptable results with few outliers, although its application is limited in $f_c \leq 80$ MPa. The prediction performance from the Goode and Narayanan [24] model significantly underestimates the axial compressive capacity of CFST, while the Giakoumelis and Lam [25] model tends to provide overestimated outputs.

Fig. 16(b) presents a comparison of predictive performance with respect to f_y. We observed that the prediction outputs of the developed NGBoost model align well with the actual test values, except for some cases when f_y is around 400 MPa and 520 MPa. Particularly for ultra-high yield strength of the steel tube ($f_y > 800$ MPa), the proposed model provides nearly perfect predictions, indicating its capability for applications involving high-strength concrete filled in high-strength steel tubes, which goes beyond the limitations of current code provisions.

In the case of EC4, although the provision limits its application to $f_y \leq 460$ MPa, the predictions generally agree well with the actual values. For the AS2327 provisions, the limitation is set at $f_y \leq 690$ MPa. However, there are some noticeable overestimated predictions when $f_y < 400$ MPa, whereas when f_y is greater than 690 MPa, the provision provides acceptable prediction accuracy. The prediction performance for the AISC code with respect to f_y is similar, characterized by evident underestimations for lower strength. However, the GB code predictions show less bias with observed outliers when $f_y \cong 400$ MPa. The predictions from the Goode and Narayanan [24] model demonstrate unacceptable underestimations across the entire range of f_y. The performance of the Giakoumelis and Lam [25] model is similar to that of the AISC code provisions.

Fig. 16(c) presents a comparison of predictive performance with respect to the D/t. It is observed that most data points fall within $D/t \leq 100$. For the developed NGBoost model, the predictions align well with the actual values, with the majority of outliers occurring when $D/t < 30$. A similar trend is observed for the performance of EC4, with outliers in the range of $D/t \leq 10$, indicating a possible disadvantage for heavily confined CFST columns.

The AISC code provisions slightly underestimate the outputs within its application range ($D/t \leq \sqrt{8E_s/f_y}$), while AS2327 shows less biased prediction performance. The GB code provides evidently better predictions for higher D/t than that when $D/t < 50$, indicating that this code exhibits more accurate prediction for lower ratio of steel tube to CFST. The Goode and Narayanan [24] model significantly underestimates the axial capacity when D/t is lower than 100, but the underestimation is less pronounced for higher D/t. Conversely, predictions from the Giakoumelis and Lam [25] model tend to overestimate the axial capacity, especially for lower D/t.

Table 4
Performance metrics (see Eq. (2)) of the NGBoost - L$\mathcal{N}(\mu, \sigma^2)$ ML model, four code based results and two existing models for the axial compressive capacity of CFST. The basic units of the performance metrics are the same as those for y_i and $\hat{y}_i$, i.e., kN.

Model	RMSE	MAE	MAPE	MedAE	R^2
NGBoost - L$\mathcal{N}(\mu, \sigma^2)$	248.09	87.93	0.0557	34.62	0.9949
Eurocode 4 [21]	486.78	255.99	0.1208	107.00	0.9874
AS/NZS 2327 [22]	671.37	339.42	0.1874	145.48	0.9677
AISC 360 [23]	884.91	400.03	0.2141	166.13	0.9328
GB 50936 [71]	362.78	207.97	0.1269	99.83	0.9893
Goode and Narayanan [24]	2426.68	1141.85	1.0401	552.56	0.2354
Giakoumelis and Lam [25]	877.30	458.10	0.1982	213.34	0.9575

The predictive performance with respect to the slenderness ratio (λ) is presented in Fig. 16(d). The predictions from the developed NGBoost model generally agree well with the actual test values when $\lambda < 80$. However, they tend to overestimate the axial capacity for higher values of λ. In the case of predictions provided by the EC4 provision, it exhibits relatively better prediction performance for lower λ compared to higher ones. The predictions are generally lower than the experimentally tested results when λ is greater than 80, indicating that the provision overestimates the reduction effects of local or global buckling. On the other hand, the predictions from the AISC provision tend to underestimate the axial compressive capacity for lower λ, while overestimating it for higher λ. This discrepancy can be attributed to the absence of consideration of confinement and buckling effects for CFST columns with low and high λ values, respectively. Chinese GB code provides general better predictions than other code provisions and models, though some outliers can be observed due to the underestimation. This may be attributed to the reduction coefficient in GB code for slender CFST columns. The prediction performance of the AS/NZS 2327 [22] and Giakoumelis and Lam [25] model shows a similar pattern, evidently overestimating the axial compressive capacity for higher values of λ. In contrast, the Goode and Narayanan [24] model provides a remarkable underestimation of predictions when λ is lower than 60.

6. Conclusions

This study aimed to develop a robust and accurate machine learning (ML) model to predict the axial compressive capacity of Concrete Filled Steel Tube (CFST) columns. We employed the Natural Gradient Boosting (NGBoost) algorithm with a LogNormal distribution, leveraging a comprehensive database of experimentally tested CFST specimens. Through extensive validation and comparison with existing code provisions and theoretical models, we established the efficacy and superiority of the proposed ML model. The key findings and implications of this research are summarized as follows:

- The NGBoost model with a LogNormal distribution demonstrated superior accuracy in predicting the axial compressive capacity of CFST columns compared to other ML models, including XGBoost, ANN, and XGBD with Normal and LogNormal distributions. The NGBoost model consistently provided high prediction confidence and minimized overfitting, making it a reliable tool for practical engineering applications. This model's performance underscores the potential of advanced ML algorithms in structural engineering predictions, surpassing traditional deterministic approaches.

- The predictive performance of the NGBoost model was benchmarked against widely used design codes such as European Code 4 (EC4), American Institute of Steel Construction (ANSI/AISC 360-22), and Australia/New Zealand Standard (AS/NZS 2327). The NGBoost model outperformed these code provisions, especially beyond their material and geometric limits. This indicates that the NGBoost model can effectively address the limitations of conventional design practices, providing accurate predictions for modern engineering requirements involving high-strength materials and larger cross-sections.
- A comprehensive database consisting of 1127 data points from experimental tests was compiled to validate the developed models. The extensive validation process included multiple performance metrics (RMSE, MAE, MAPE, MedAE, and R^2), which confirmed the robustness and accuracy of the NGBoost model in both point and probabilistic predictions. This thorough validation ensures the reliability of the model for diverse design scenarios.
- SHAP analysis revealed the significant influence of geometric parameters, particularly the diameter (D) and length (L) of the CFST column, on the axial compressive capacity predictions. This emphasizes the importance of these parameters in the design and optimization of CFST columns. The analysis also highlighted the relative importance of other features such as thickness (t), load eccentricity (e), compressive strength of concrete (f_c), and yield strength of steel (f_y), providing valuable insights for structural engineers.
- The parametric study offered valuable insights into the effects of varying key input features (D, t, L, e, f_c, and f_y) on the predicted axial compressive capacity. The findings highlight the critical role of optimizing cross-sectional dimensions and material strengths to achieve desired structural performance. The contour plots generated from the parametric study serve as practical tools for engineers to make informed design decisions, ensuring efficient and safe CFST column configurations.

In conclusion, the NGBoost model with a LogNormal distribution represents a significant advancement in the predictive modeling of CFST columns. Its ability to provide accurate and probabilistic predictions makes it a valuable tool for engineers, offering enhanced design reliability and performance assessment. The success of this model underscores the potential of integrating advanced ML techniques into structural engineering practices. Future research could explore the integration of additional features, the application of this model to other types of composite structures, and the extension of this approach to dynamic loading conditions, further broadening its applicability and utility in the field of structural engineering.

CRediT authorship contribution statement

Dade Lai: Writing – original draft, Software, Data curation. **Jingyu Wei:** Writing – review & editing, Resources, Data curation. **Alessandro Contento:** Writing – review & editing, Methodology, Data curation. **Junqing Xue:** Writing – review & editing, Resources, Data curation. **Bruno Briseghella:** Writing – review & editing, Project administration. **Tommaso Albanesi:** Writing – review & editing, Methodology. **Cristoforo Demartino:** Writing – review & editing, Supervision, Investigation.

Declaration of competing interest

The authors declare that they have no known competing financial interests or personal relationships that could have appeared to influence the work reported in this paper.

Acknowledgments

This work has been supported by National Natural Science Foundation of China (NSFC, 52408161 and W2433120). The study presented was carried out as part of the program of activities carried out as part of the agreement between the ReLUIS Interuniversity Consortium and the Superior Council of Public Works stipulated pursuant to art. 3 of the Decree of the Minister of Infrastructure no. 578 of 17 December 2020; however, this publication does not necessarily reflect the Council's position and assessments.

Appendix A. Summary of collected data

See Fig. A.17.

Appendix B. Review of available predictive models

The determination of axial compressive load capacity of CFST columns is essential for ensuring the structural integrity and safety of engineering designs. Various standard code provisions and theoretical models have been developed to predict this capacity. This section provides a review of widely used standards and models, including the European Code 4 (EC4), the American Institute of Steel Construction (ANSI/AISC 360-22), and the Australia/New Zealand Standard (AS/NZS 2327) (Appendix B.1). Additionally, theoretical models proposed by Goode and Narayanan [24] and Giakoumelis and Lam [25] are discussed (Appendix B.2).

B.1. Standards and code of practice

B.1.1. Eurocode 4 (EC4)

For circular CFST column sections, the sectional strength is determined by considering the capacity of both the inner concrete and the outer steel tube:

$$N_{uc}^{EC4} = A_s f_y + A_c f_c \tag{B.1}$$

where A_s and A_c are the section areas of outer steel tube and inner concrete, respectively. When the relative slenderness, $\bar{\lambda} \le 0.5$, and the eccentricity ratio, $e/D \le 0.1$, are met, the circular CFST column is assumed to benefit from the steel tube's confinement effect, and the sectional capacity is calculated considering this effect:

$$N_{uc}^{EC4} = \eta_s A_s f_y + \left(1 + \eta_c \frac{t}{D}\frac{f_y}{f_c}\right) A_c f_c \tag{B.2}$$

where:

$$\eta_s = \eta_{s0} + \left(1 - \eta_{s0}\right)\frac{10e}{D} \tag{B.3a}$$

$$\eta_c = \eta_{c0}\left(1 - \frac{10e}{D}\right) \tag{B.3b}$$

$$\eta_{s0} = 0.25\left(3 + 2\bar{\lambda}\right) \le 1 \tag{B.3c}$$

$$\eta_{c0} = 4.9 - 18.5\bar{\lambda} + 17\bar{\lambda}^2 \ge 0 \tag{B.3d}$$

Here, η_s and η_c are two coefficients consider the steel tube confinement effects; η_{s0} accounts for the reduction of the capacity of steel tube due to lateral expansion of inner concrete, and η_{c0} denotes the enhancement of the capacity of inner concrete from confinement effects. The relative slenderness, $\bar{\lambda}$, in EC4 [21] is defined by the following equation:

$$\bar{\lambda} = \sqrt{\frac{N_{ns}}{N_{cr}}} \tag{B.4}$$

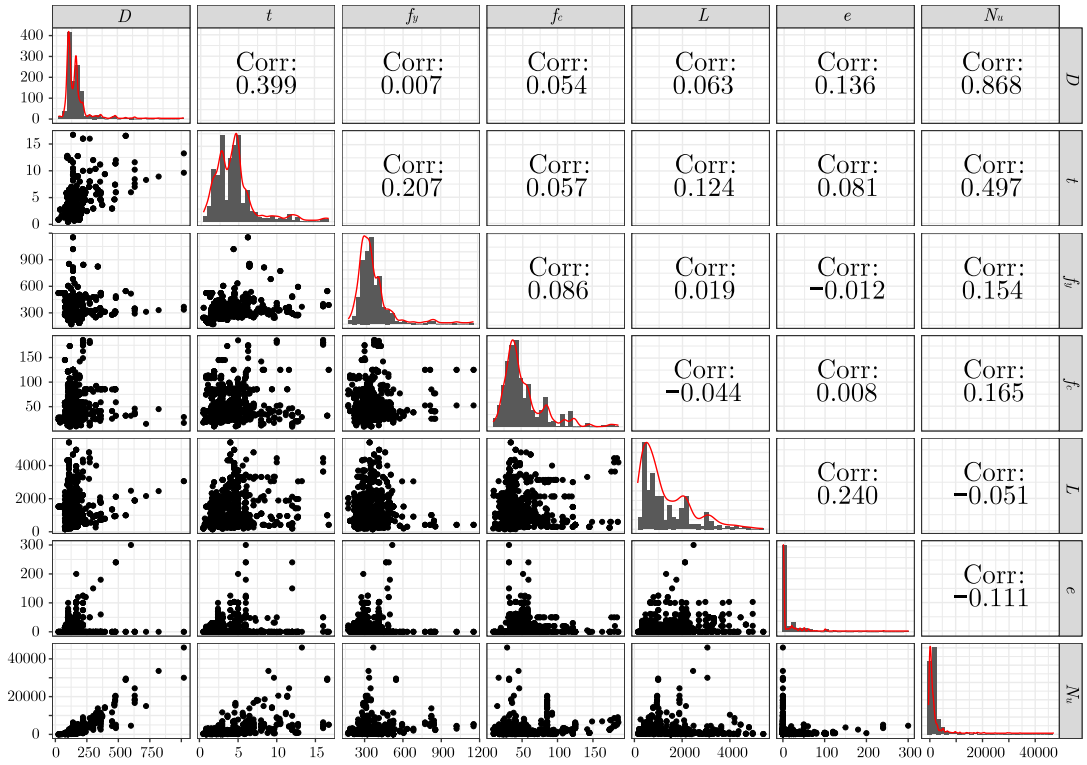

Fig. A.17. Pair plot matrix of the database. The diagonal of the matrix represents the distribution curve (histogram and pdf). The lower segment of the matrix showcases scatter pair plots, visually depicting the interrelationships between each pair of variables. Conversely, the upper segment of the matrix displays the Pearson correlation coefficient (r) quantifying the strength and direction of association between the corresponding two features or between a feature and the target variable.

where $N_{ns} = A_s f_y + A_c f_c$ is the unconfined strength of CFST column, and N_{cr} represents the buckling strength of CFST column, which can be determined by:

$$N_{cr}^{EC4} = \frac{\pi^2 EI^{EC4}}{L_e} \tag{B.5a}$$

$$EI^{EC4} = E_s I_s + 0.6 E_c^{EC4} I_c \tag{B.5b}$$

$$E_c^{EC4} = 22\left(\frac{f_c + 8}{10}\right)^{0.3} \tag{B.5c}$$

where L_e and EI are the effective length of the CFST column and effective buckling strength. The moments of area I_s and I_c represent the second moments of the steel and concrete sections, respectively. E_s and E_c are the elastic moduli of the steel and concrete materials. The factor 0.6 aims to consider the cracking reduction effects of the concrete.

The CFST column member strength is calculated based on the sectional strength combined with a reduction factor χ to account for potential global buckling:

$$N_u^{EC4} = \chi N_{uc}^{EC4} \tag{B.6a}$$

$$\chi = \frac{1}{\phi + \sqrt{\phi^2 - \bar{\lambda}^2}} \leq 1 \tag{B.6b}$$

$$\phi = 0.5\left[1 + 0.21\left(\bar{\lambda} - 0.2\right) + \bar{\lambda}^2\right] \tag{B.6c}$$

It should be noted that the EC4 code provisions [21] limit its application under the following conditions:

$$\begin{cases} f_c \leq 60 \text{ MPa} \\ f_y \leq 460 \text{ MPa} \\ \frac{D}{t} \leq 90\frac{235}{f_y} \end{cases} \tag{B.7}$$

B.1.2. Australia standard/New Zealand standard 2327 (AS2327)

The AS/NZS 2327 code [22] provides similar calculation provisions to EC4 [21] for the axial compressive capacity of CFST columns, with primary differences in accounting for local buckling effects. In AS/NZS 2327 [22], local buckling is calculated using a coefficient k_f that considers an effective width method to reduce the steel tube's contribution. The sectional strength is then determined using:

$$N_{uc}^{AS} = k_f A_s f_y + A_c f_c \tag{B.8}$$

The enhancement of circular CFST columns with confinement effects is expressed as:

$$N_{uc}^{AS} = k_f \eta_s A_s f_y + \left(1 + \eta_c \frac{t}{D}\frac{f_y}{f_c}\right) A_c f_c \tag{B.9}$$

where the local buckling reduced factor, k_f is defined as the effective area ratio to the gross section area:

$$k_f = \frac{A_e}{A_g} = \frac{\pi\left(D_e t - t^2\right)}{4\left(A_s + A_c\right)} \tag{B.10a}$$

$$D_e = \min\left(D\sqrt{\frac{\lambda_{ey}}{\bar{\lambda}}}, D\left(\frac{3\lambda_{ey}}{\bar{\lambda}}\right)\right) \leq D \tag{B.10b}$$

$$\lambda_{ey} = 3\sqrt{\frac{E_s}{f_y}} \tag{B.10c}$$

The buckling strength of CFST N_{cr} and the relative slenderness $\bar{\lambda}$ are calculate using the same equation as EC4 [21] (see Eqs. (B.4) and (B.5a)). However, the methods for calculating effective flexural stiffness and the elastic modulus of concrete differ, given by:

$$EI^{AS} = E_s I_s + E_c^{AS} I_c \tag{B.11a}$$

$$E_c^{AS} = \begin{cases} \rho_c^{1.5} 0.043\sqrt{f_{cmi}} & \text{if } f_{cmi} \leq 40 \text{ MPa} \\ \rho_c^{1.5}\left(0.024\sqrt{f_{cmi}} + 0.12\right) & \text{if } f_{cmi} > 40 \text{ MPa} \end{cases} \tag{B.11b}$$

$$f_{cmi} = 0.9 f_c \left(1.2875 - 0.001875 f_c\right) \tag{B.11c}$$

where f_{cmi} represents the mean value of the compressive strength of concrete and $\rho_c = 2400$ kg/m^3 is the density of the concrete. The member strength of a CFST column under axial compressive load, according to AS2327 provisions, is calculated as follows:

$$N_u^{AS} = \alpha_c N_{uc}^{AS} \tag{B.12a}$$

$$\alpha_c = \xi \left[1 - \sqrt{1 - \left(\frac{90}{\xi \lambda_\alpha}\right)^2}\right] \tag{B.12b}$$

$$\xi = \frac{\left(\lambda_\alpha/90\right)^2 + 1 + \eta}{2\left(\lambda_\alpha/90\right)^2} \tag{B.12c}$$

$$\lambda_\alpha = \lambda_\eta + \alpha_a \alpha_b \tag{B.12d}$$

$$\lambda_\eta = 90\bar{\lambda} \tag{B.12e}$$

$$\eta = 0.00326\left(\lambda - 13.5\right) \tag{B.12f}$$

$$\alpha_a = \frac{2100\left(\lambda_\eta - 13.5\right)}{\lambda_\eta^2 - 15.3\lambda_\eta + 2050} \tag{B.12g}$$

$$\alpha_b = \begin{cases} 0 & \text{if } k_f < 1 \\ 1 & \text{if } k_f = 1 \end{cases} \tag{B.12h}$$

The limitation of AS2327 provisions are given by:

$$\begin{cases} f_c \le 100 \text{ MPa} \\ f_y \le 690 \text{ MPa} \\ \frac{D}{t} \le 0.19\frac{E_s}{f_y} \end{cases} \tag{B.13}$$

B.1.3. American Institute of Steel Construction (ANSI/AISC 360-22)

Similar to EC4 [21], for compact circular section, the sectional strength of CFST column in AISC code is designed based on the capacity of inner concrete and outer steel tube:

$$N_{uc}^{AISC} = A_s f_y + 0.95 A_c f_c \tag{B.14}$$

The member strength of CFST column under axial compressive load is calculated using following equations:

$$N_u^{AISC} = \begin{cases} N_{uc}^{AISC}\left(0.658^{N_{uc}^{AISC}/N_{cr}^{AISC}}\right) & \text{if } \frac{N_{uc}^{AISC}}{N_{cr}^{AISC}} \le 2.25 \\ 0.877 N_{cr}^{AISC} & \text{if } \frac{N_{uc}^{AISC}}{N_{cr}^{AISC}} > 2.25 \end{cases} \tag{B.15}$$

where N_{cr}^{AISC} is calculated using same equation as EC4 [21] (Eq. (B.5a)), while the effective flexural stiffness, EI and the elastic modulus of concrete, E_c are given by:

$$EI^{AISC} = E_s I_s + \varphi E_c^{AISC} I_c \tag{B.16a}$$

$$\varphi = 0.45 + 3\frac{A_s}{A_s + A_c} \le 0.9 \tag{B.16b}$$

$$E_c^{AISC} = 0.043 \rho_c^{1.5} \sqrt{f_c} \tag{B.16c}$$

The valid applicable conditions are $f_c \le 69$ MPa, $f_y \le 525$ MPa, and $D/t \le \sqrt{8E_s/f_y}$.

B.1.4. Chinese standard (GB50936-2014)

According to Chinese CFST standard, the axial compressive capacity design value for circular CFST column can be calculated based the following equation.

$$N_u^{GB} = \phi_e \phi_l N_0 \tag{B.17}$$

where N_0 is the axial compressive capacity for CFST without reduction, and it is calculated from:

$$N_0 = \begin{cases} 0.9 A_c f_c \left(1 + \alpha\theta\right) & \theta \le \frac{1}{(\alpha-1)^2} \\ 0.9 A_c f_c \left(1 + \sqrt{\theta} + \theta\right) & \theta > \frac{1}{(\alpha-1)^2} \end{cases} \tag{B.18}$$

where $\theta = A_s f_y / A_c f_c$ is the reinforcement ratio from steel tube; α is a coefficient related on the concrete strength for $f_c \le 80$ MPa. ϕ_e and ϕ_l are two reduction factors for eccentric load and slender columns, respectively. These two factors are calculated from:

$$\phi_e = \begin{cases} \frac{1}{1+1.85\frac{e}{r_c}} & \frac{e}{r_c} \le 1.55 \\ \frac{1}{3.92 - 5.16\phi_l + \phi_l \frac{e}{0.3 r_c}} & \frac{e}{r_c} > 1.55 \end{cases} \tag{B.19}$$

$$\phi_l = \begin{cases} 1 - 0.115\sqrt{\frac{L}{D} - 4} & \frac{L}{D} > 30 \\ 1 - 0.0226\left(\frac{L}{D} - 4\right) & 4 < \frac{L}{D} \le 30 \\ 1 & \frac{L}{D} \le 4 \end{cases} \tag{B.20}$$

where r_c is the radius of the inner concrete.

B.2. Theoretical models

B.2.1. Goode and Narayanan (1997)

Goode and Narayanan [24] proposed the following equation to calculate the axial compressive load capacity of CFST columns:

$$N_u = \frac{6t}{D - 2t} A_s f_y + 0.85 A_c f_c \tag{B.21}$$

B.2.2. Giakoumelis and Lam (2004)

Giakoumelis and Lam [25] proposed a model for predicting the axial compressive capacity of CFST columns, expressed as:

$$N_u = A_s f_y + 1.3 A_c f_c \tag{B.22}$$

Data availability

The data that support the findings of this study are available from the corresponding author upon reasonable request.

References

[1] AlHamaydeh M, Ghazal Aswad N. Structural health monitoring techniques and technologies for large-scale structures: Challenges, limitations, and recommendations. Pract Period Struct Des Constr 2022;27(3):03122004.

[2] Lee CH, Kang KY, Kim SY, Koo CH. Review of structural design provisions of rectangular concrete filled tubular columns. J Korean Soc Steel Constr 2013;25(4):389–98.

[3] Huang Y, Briseghella B, Zordan T, Wu Q, Chen B. Shaking table tests for the evaluation of the seismic performance of an innovative lightweight bridge with CFST composite truss girder and lattice pier. Eng Struct 2014;75:73–86.

[4] Huang W, Fenu L, Chen B, Briseghella B. Experimental study on K-joints of concrete-filled steel tubular truss structures. J Constr Steel Res 2015;107:182–93.

[5] Huang W, Fenu L, Chen B, Briseghella B. Experimental study on joint resistance and failure modes of concrete filled steel tubular (CFST) truss girders. J Constr Steel Res 2018;141:241–50.

[6] Yadav R, Yuan H, Chen B, Lian Z. Experimental study on seismic performance of latticed CFST-RC column connected with RC web. Thin-Walled Struct 2018;126:258–65.

[7] Zheng J, Wang J. Concrete-filled steel tube arch bridges in China. Engineering 2018;4(1):143–55.

[8] Ferrotto MF, Fenu L, Xue J-Q, Briseghella B, Chen B-C, Cavaleri L. Simplified equivalent finite element modelling of concrete-filled steel tubular K-joints with and without studs. Eng Struct 2022;266:114634.

[9] He F, Li C, Chen B, Briseghella B, Xue J. Axial compression behavior of steel tube reinforced concrete column. Eng Struct 2024;303:117548.

[10] Han L-H, Li W, Bjorhovde R. Developments and advanced applications of concrete-filled steel tubular (CFST) structures: Members. J Constr Steel Res 2014;100:211–28.

[11] Ren Q-X, Han L-H, Lam D, Hou C. Experiments on special-shaped CFST stub columns under axial compression. J Constr Steel Res 2014;98:123–33.

[12] Evirgen B, Tuncan A, Taskin K. Structural behavior of concrete filled steel tubular sections (CFT/CFSt) under axial compression. Thin-Walled Struct 2014;80:46–56.

[13] Ren Z, Wang D, Li P. Axial compressive behaviour and confinement effect of round-ended rectangular CFST with different central angles. Compos Struct 2022;285:115193.

[14] De Oliveira WLA, De Nardin S, de Cresce El ALH, El Debs MK, et al. Influence of concrete strength and length/diameter on the axial capacity of CFT columns. J Constr Steel Res 2009;65(12):2103–10.

[15] De Nardin S, El Debs ALHd. Axial load behaviour of concrete-filled steel tubular columns. Proc Inst Civ Eng-Struct Build 2007;160(1):13–22.
[16] Xue J-Q, Briseghella B, Chen B-C. Effects of debonding on circular CFST stub columns. J Constr Steel Res 2012;69(1):64–76.
[17] Xue J-Q, Fiore A, Liu Z-H, Briseghella B, Marano GC. Prediction of ultimate load capacities of CFST columns with debonding by EPR. Thin-Walled Struct 2021;164:107912.
[18] Contento A, Aloisio A, Xue J, Quaranta G, Briseghella B, Gardoni P. Probabilistic axial capacity model for concrete-filled steel tubes accounting for load eccentricity and debonding. Eng Struct 2022;268:114730.
[19] Xue J-Q, Huang J-P, Fiore A, Briseghella B, Marano GC. Prediction of the mechanical performance of compressed circular CFST columns with circumferential debonding gap. J Constr Steel Res 2023;208:107988.
[20] Wang W, Tang Z, Li Z, Ma H, et al. Bearing capacities of different-diameter concrete-filled steel tubes under axial compression. Adv Mater Sci Eng 2016;2016.
[21] 4 E. Design of composite steel and concrete structures. Part 1.1, General rules and rules for buildings. European Committee for Standardization; 2004.
[22] AS/NZS. Composite structures–composite steel-concrete construction buildings. Australia Standard; 2017.
[23] AISC. Specification for structural steel buildings ANSI/AISC 360-16. American Institute of Steel Construction; 2022.
[24] Goode C, Narayanan R. Design of concrete filled steel tubes to EC4. In: Proceedings of the ASCCS seminar on concrete filled steel tubes a comparison of international codes and practice, innsbruck, Austria. 1997, p. 1–25.
[25] Giakoumelis G, Lam D. Axial capacity of circular concrete-filled tube columns. J Constr Steel Res 2004;60(7):1049–68.
[26] Sakino K, Nakahara H, Morino S, Nishiyama I. Behavior of centrally loaded concrete-filled steel-tube short columns. J Struct Eng 2004;130(2):180–8.
[27] Han L-H, Yao G-H, Zhao X-L. Tests and calculations for hollow structural steel (HSS) stub columns filled with self-consolidating concrete (SCC). J Constr Steel Res 2005;61(9):1241–69.
[28] Du Y, Chen Z, Xiong M-X. Experimental behavior and design method of rectangular concrete-filled tubular columns using Q460 high-strength steel. Constr Build Mater 2016;125:856–72.
[29] Wang Z-B, Tao Z, Han L-H, Uy B, Lam D, Kang W-H. Strength, stiffness and ductility of concrete-filled steel columns under axial compression. Eng Struct 2017;135:209–21.
[30] Wei J, Luo X, Lai Z, Varma AH. Experimental behavior and design of high-strength circular concrete-filled steel tube short columns. J Struct Eng 2020;146(1):04019184.
[31] Wei J, Xie Z, Zhang W, Luo X, Yang Y, Chen B. Experimental study on circular steel tube-confined reinforced UHPC columns under axial loading. Eng Struct 2021;230:111599.
[32] Faridmehr I, Nehdi ML, Nejad AF, Sahraei MA, Kamyab H, Valerievich KA. An innovative multi-objective optimization approach for compact concrete-filled steel tubular (CFST) column design utilizing lightweight high-strength concrete. Int J Lightweight Mater Manuf 2024.
[33] Reich Y. Machine learning techniques for civil engineering problems. Comput-Aided Civ Infrastruct Eng 1997;12(4):295–310.
[34] Thai H-T. Machine learning for structural engineering: A state-of-the-art review. In: Structures. Vol. 38, Elsevier; 2022, p. 448–91.
[35] Deka PC. A primer on machine learning applications in civil engineering. CRC Press; 2019.
[36] Falcone R, Lima C, Martinelli E. Soft computing techniques in structural and earthquake engineering: a literature review. Eng Struct 2020;207:110269.
[37] Di Trapani F, Sberna AP, Marano GC. A new genetic algorithm-based framework for optimized design of steel-jacketing retrofitting in shear-critical and ductility-critical RC frame structures. Eng Struct 2021;243:112684.
[38] Di Trapani F, Sberna AP, Marano GC. A genetic algorithm-based framework for seismic retrofitting cost and expected annual loss optimization of non-conforming reinforced concrete frame structures. Comput Struct 2022;271:106855.
[39] Sberna AP, Demartino C, Vanzi I, Marano GC, Di Trapani F. Cost-effective topology optimization of masonry structure reinforcements by a linear static analysis-based GA framework. Bull Earthq Eng 2024;1–25.
[40] Ahmadi M, Naderpour H, Kheyroddin A. Utilization of artificial neural networks to prediction of the capacity of CCFT short columns subject to short term axial load. Arch Civ Mech Eng 2014;14(3):510–7.
[41] Ahmadi M, Naderpour H, Kheyroddin A. ANN model for predicting the compressive strength of circular steel-confined concrete. Int J Civ Eng 2017;15:213–21.
[42] Tran V-L, Thai D-K, Nguyen D-D. Practical artificial neural network tool for predicting the axial compression capacity of circular concrete-filled steel tube columns with ultra-high-strength concrete. Thin-Walled Struct 2020;151:106720.
[43] Du Y, Chen Z, Zhang C, Cao X. Research on axial bearing capacity of rectangular concrete-filled steel tubular columns based on artificial neural networks. Front Comput Sci 2017;11:863–73.
[44] Tran V-L, Thai D-K, Kim S-E. Application of ANN in predicting ACC of SCFST column. Compos Struct 2019;228:111332.
[45] Zarringol M, Thai H-T, Thai S, Patel V. Application of ANN to the design of CFST columns. In: Structures. Vol. 28, Elsevier; 2020, p. 2203–20.
[46] Ngo N-T, Nguyen Q-T, Huynh V-V, et al. Prediction of axial strength in circular steel tube confined concrete columns using artificial intelligence. J Sci Technol Civ Eng (STCE)-HUCE 2021;15(2):113–26.
[47] Ngo N-T, Le HA, Pham T-P-T. Integration of support vector regression and grey wolf optimization for estimating the ultimate bearing capacity in concrete-filled steel tube columns. Neural Comput Appl 2021;33:8525–42.
[48] Lyu F, Fan X, Ding F, Chen Z. Prediction of the axial compressive strength of circular concrete-filled steel tube columns using sine cosine algorithm-support vector regression. Compos Struct 2021;273:114282.
[49] Tran V-L, Kim S-E. Efficiency of three advanced data-driven models for predicting axial compression capacity of CFDST columns. Thin-Walled Struct 2020;152:106744.
[50] Le T-T, Phan HC. Prediction of ultimate load of rectangular CFST columns using interpretable machine learning method. Adv Civ Eng 2020;2020:1–16.
[51] Zhou X-G, Hou C, Feng W-Q. Optimized data-driven machine learning models for axial strength prediction of rectangular CFST columns. In: Structures. Vol. 47, Elsevier; 2023, p. 760–80.
[52] Vu Q-V, Truong V-H, Thai H-T. Machine learning-based prediction of CFST columns using gradient tree boosting algorithm. Compos Struct 2021;259:113505.
[53] Lee S, Vo TP, Thai H-T, Lee J, Patel V. Strength prediction of concrete-filled steel tubular columns using Categorical Gradient Boosting algorithm. Eng Struct 2021;238:112109.
[54] Goulet J-A. Probabilistic machine learning for civil engineers. MIT Press; 2020.
[55] Feng D-C, Chen S-Z, Azadi Kakavand MR, Taciroglu E. Probabilistic model based on Bayesian model averaging for predicting the plastic hinge lengths of reinforced concrete columns. J Eng Mech 2021;147(10):04021066.
[56] Zhang J, Wan C, Sato T. Advanced Markov chain Monte Carlo approach for finite element calibration under uncertainty. Comput-Aided Civ Infrastruct Eng 2013;28(7):522–30.
[57] Duan T, Anand A, Ding DY, Thai KK, Basu S, Ng A, Schuler A. Ngboost: Natural gradient boosting for probabilistic prediction. In: International conference on machine learning. PMLR; 2020, p. 2690–700.
[58] Chen S-Z, Feng D-C, Wang W-J, Taciroglu E. Probabilistic machine-learning methods for performance prediction of structure and infrastructures through natural gradient boosting. J Struct Eng 2022;148(8):04022096.
[59] Mei Y, Sun Y, Li F, Xu X, Zhang A, Shen J. Probabilistic prediction model of steel to concrete bond failure under high temperature by machine learning. Eng Fail Anal 2022;142:106786.
[60] Chen T, Guestrin C. Xgboost: A scalable tree boosting system. In: Proceedings of the 22nd acm sigkdd international conference on knowledge discovery and data mining. 2016, p. 785–94.
[61] Flood I. Towards the next generation of artificial neural networks for civil engineering. Adv Eng Inform 2008;22(1):4–14.
[62] Donnerer C. 2021. URL: https://github.com/CDonnerer/xgboost-distribution.
[63] Schmidhuber J. Deep learning in neural networks: An overview. Neural Netw. 2015;61:85–117.
[64] Martinez-Cantin R. BayesOpt: a Bayesian optimization library for nonlinear optimization, experimental design and bandits.. J Mach Learn Res 2014;15(1):3735–9.
[65] Gulli A, Pal S. Deep learning with Keras. Packt Publishing Ltd; 2017.
[66] Chollet F. Deep learning with Python. Simon and Schuster; 2021.
[67] Lai D, Demartino C, Xiao Y. Interpretable machine-learning models for maximum displacements of RC beams under impact loading predictions. Eng Struct 2023;281:115723.
[68] Xu B, Wang N, Chen T, Li M. Empirical evaluation of rectified activations in convolutional network. 2015, arXiv preprint arXiv:1505.00853.
[69] Taylor KE. Summarizing multiple aspects of model performance in a single diagram. J Geophys Res: Atmos 2001;106(D7):7183–92.
[70] Lundberg SM, Lee S-I. A unified approach to interpreting model predictions. Adv Neural Inf Process Syst 2017;30.
[71] GB50936. Technical code for concrete filled steel tubular structures. Natl Stand of P.R.C 2014.